AD NUMBER
ADB009982
LIMITATION CHANGES
TO: **Approved for public release; distribution is unlimited.**
FROM: **Distribution authorized to U.S. Gov't. agencies only; Test and Evaluation; FEB 1976. Other requests shall be referred to Army Ballistic Research Laboratory, Attn: DRXBR-SS, Aberdeen Proving Ground, MD 21005.**
AUTHORITY
usaardc ltr, 31 may 1978

THIS REPORT HAS BEEN DELIMITED
AND CLEARED FOR PUBLIC RELEASE
UNDER DOD DIRECTIVE 5200.20 AND
NO RESTRICTIONS ARE IMPOSED UPON
ITS USE AND DISCLOSURE.

DISTRIBUTION STATEMENT A

APPROVED FOR PUBLIC RELEASE;
DISTRIBUTION UNLIMITED.

AD

BRL MR 2588

BRL

MEMORANDUM REPORT NO. 2588

(Supersedes IMR No. 379)

AD B009982

WIND TUNNEL EXPERIMENTS OF THE EFFECT OF NEAR-WAKE COMBUSTION ON THE BASE DRAG OF SUPERSONIC PROJECTILES

J. Richard Ward
Frank P. Baltakis
Theresa A. Elmendorf
Dennis J. Mancinelli

February 1976

AD No.
DDC FILE COPY

Distribution limited to US Government agencies only; Test and Evaluation; Feb 1976. Other requests for this document must be referred to Director, USA Ballistic Research Laboratories, ATTN: DRXBR-SS, Aberdeen Proving Ground, Maryland 21005.

USA BALLISTIC RESEARCH LABORATORIES
ABERDEEN PROVING GROUND, MARYLAND

UNCLASSIFIED

SECURITY CLASSIFICATION OF THIS PAGE (When Data Entered)

REPORT DOCUMENTATION PAGE | READ INSTRUCTIONS BEFORE COMPLETING FORM

1. REPORT NUMBER: BRL MEMORANDUM REPORT NO. 2588 (14) BRL-MR-2588
2. GOVT ACCESSION NO.
3. RECIPIENT'S CATALOG NUMBER

4. TITLE (and Subtitle): (6) "Wind Tunnel Experiments of the Effect of Near-Wake Combustion on the Base Drag of Supersonic Projectiles".
5. TYPE OF REPORT & PERIOD COVERED: (9) Memorandum Report,
6. PERFORMING ORG. REPORT NUMBER

7. AUTHOR(s): (10)
J. Richard Ward,
Frank P. Baltakis,
Theresa A. Elmendorf Dennis J. Mancinelli
8. CONTRACT OR GRANT NUMBER(s)

9. PERFORMING ORGANIZATION NAME AND ADDRESS:
US Army Ballistic Research Laboratories
Aberdeen Proving Ground, MD 21005
10. PROGRAM ELEMENT, PROJECT, TASK AREA & WORK UNIT NUMBERS: Project No. 1F262201DH96

11. CONTROLLING OFFICE NAME AND ADDRESS:
U. S. Army Materiel Development & Research Command
5001 Eisenhower Avenue
Alexandria, VA 22333
12. REPORT DATE: (11) FEBRUARY 1976
13. NUMBER OF PAGES: (12) 72 p.

14. MONITORING AGENCY NAME & ADDRESS (if different from Controlling Office): (16) DA-1-F-262201-DH-96
15. SECURITY CLASS. (of this report): Unclassified
15a. DECLASSIFICATION/DOWNGRADING SCHEDULE

16. DISTRIBUTION STATEMENT (of this Report)
Distribution limited to US Government agencies only; Test and Evaluation; February 1976. Other requests for this document must be referred to Director, USA Ballistic Research Laboratories, ATTN: DRXBR-SS, Aberdeen Proving Ground, Maryland 21005.

17. DISTRIBUTION STATEMENT (of the abstract entered in Block 20, if different from Report)

18. SUPPLEMENTARY NOTES

Supersedes BRL IMR No. 379

19. KEY WORDS (Continue on reverse side if necessary and identify by block number)
base drag reduction, base pressure, aerodynamic combustion, fumers, pyrotechnics, tracers, ammunition effectiveness, automatic cannon

20. ABSTRACT (Continue on reverse side if necessary and identify by block number) ssv/4589

A series of fumers based on magnesium/strontium peroxide was tested at the Naval Surface Weapon Center's Hypersonic Tunnel to see the effect of varying the parameters that control the rate of combustion of pyrotechnics. The parameters that were varied included spin rate, fuel content, fuel particle size, the oxidizer, and the addition of burning rate additives (calcium resinate, polyvinylchloride, oxamide, and gelatin). The base drag reductions measured for all the mixes could be approximately correlated by a single expression

(continued on reverse side) Dm

DD FORM 1 JAN 73 1473 EDITION OF 1 NOV 65 IS OBSOLETE

UNCLASSIFIED 050 750

SECURITY CLASSIFICATION OF THIS PAGE (When Data Entered)

20. ABSTRACT: (Continued)

relating base drag reduction to the mass burning rate of the fumer mix. The base drag reduction estimated for propellant combustion gases is similar to the base drag reductions achieved with pyrotechnics. This raises the possibility of "invisible" fumer mixes.

TABLE OF CONTENTS

LIST OF TABLES

LIST OF FIGURES

LIST OF SYMBOLS

M_∞	free-stream Mach number
P_b	base pressure
P_∞	free-stream static pressure
P_o	supply pressure
P	Pitot pressure
P_1 to P_8	base pressure orifices, Figure 2
T_o	supply temperature
T_∞	free-stream temperature
X	axial distance from the model base
y	radial distance from the model wall
γ	ratio of specific heats
C_{Db}	base drag coefficient
A	area
Mw	molecular weight of air
R	universal gas constant
d	diameter of the fumer cavity
m	fumer mass
t_b	fumer burning time
$\dot{m}$	average mass burning rate of the fumer
ρ	density of the fumer
I	injection parameter
$\Delta(P_b/P_\infty)$	change in P_b/P_∞ during combustion
rpm	revolutions/minute
δ	boundary layer thickness
Re	Reynolds number
ℓ	length of the wind tunnel model

I. INTRODUCTION

A systematic examination of projectile shapes[1] concluded that a longer, streamlined projectile with a length-to-diameter ratio of 5.5 would have a higher striking energy and a shorter time of flight than conventional automatic cannon or small arms projectiles.

Since the base drag compri ver half the total drag for such a streamlined projectile,[1] even h...er striker energies and shorter flight times are possible if the base drag can be eliminated.

The base drag arises from the partial vacuum at the base of a supersonic projectile. The approaches used in the past to reduce the base drag of projectiles include base geometry optimization, boundary-layer bleed into the base region, and the addition of heat and mass. A review of this previous work has recently appeared.[2]

This report deals with experiments directed towards reducing base drag by direct injection of heat and mass into the wake region. The word, "fumer", has been coined for substances designed to release heat and mass into the wake region. Work related to this new technology area is in progress in industrial, academic, and government laboratories; such work ranges from gun firings to analytical modeling of the wake region including the effect of heat and mass injection. A summary of this work is in press;[3] a description of the gun firings is discussed in a Frankford Arsenal report.[4]

Pyrotechnics have been chosen as candidate fumer compositions since it is well known that pyrotechnics will burn at atmospheric pressure and will pass military safety and storage requirements. In the experments reported here, the variables that affect the burning rate of a pyrotechnic are examined systematically to see how such variables alter fumer performance. The experiments were conducted in a wind tunnel at simulated projectile flight conditions.

II. EXPERIMENTAL

A. Test Conditions

The experiments were conducted at the Naval Surface Weapon Center's Hypersonic Tunnel that has large capacity air supply and heating systems.

---

[1] *B. J. Reiter, B. B. Grollman, and A. E. Thrailkill, "A Compendium of Ballistic Properties of Projectiles of Possible Interest in Small Arms," BRL Report No. 1532, February 1971. AD# 882117.*

[2] *S. N. B. Murthy and J. R. Osborn, "Base Flow Data With and Without Injection: Bibliography and Semi-Rational Correlations," BRL Contract Report No. 113, August 1973. AD# 914188L.*

[3] *S. N. B. Murthy, J. R. Osborn, J. R. Ward, and A. W. Barrows, eds, Aerodynamics of Base Combustion, MIT Press, Boston, in press.*

[4] *R. Kwatnoski, "Drag-Reducing Fumer for Application in Small Arms Ammunition," Frankford Arsenal Report No. R-3003, March 1974.*

The latter was necessary to achieve sea-level temperatures in the test section. Normally, this tunnel is operated at Mach numbers 5-10. Recently, it was equipped with two additional stilling chambers which permit its operation at sea-level conditions. The flow nozzle was of center-body design with a 15cm exit diameter. The test setup is illustrated in Figure 1. All experiments were done with the Mach 1.98 nozzle described previously.[5] An index is provided in Appendix A listing the fumer mix and flow conditions for each test run. This includes some data on runs done with fumer mixes supplied by Picatinny Arsenal.[6] Table I lists the constituents of all fumer mixes discussed in this report.

B. Model and Instrumentation

Projectile base flow was simulated by a cylindrical body which was supported in the settling chamber and extended through the nozzle throat into the test section. The model was 2.5cm in diameter and 27cm long when measured from the throat. Model surface was sandblasted to a roughness of about 0.01mm to ensure a turbulent boundary layer at the base. On a number of selected runs a 15cm long extension was used to increase the boundary layer thickness at the model base.

The fumer mix for each run was contained in a steel capsule in a 1.5cm, i.d., by 2.0cm deep cavity. The fumer mixes were ignited by a laser beam (250 watt CO_2 laser manufactured by Westinghouse) operated in the continuous mode. The light beam diameter at the plane of impingement was about 1cm and the exposure time varied from 2 to 5 seconds.

The model base was instrumented with eight pressure orifices arranged as in Figure 2. On test runs with the extended model only four tubes were used. Immediately after removal of the model extension (Run 123), orifice tubes P1, P2, P3, P4, P5, and P6 were extended 0.6, 1, 1, 2, 2.5, and 1cm respectively past the base for pressure measurements in the near-wake. Unfortunately, these tubes burnt off so early in a combustion run that no meaningful results were obtained.

The model was equipped with an air turbine capable of spin rates up to 50,000 rpm and with a force balance for direct base drag determination (Figure 3). Six pressure orifices were provided near the model periphery for base drag determinations during tests with spin.

Preceding the combustion tests, boundary layer measurements were made on the model surface a short distance upstream of the base. The measurements were made with a flattened Pitot-type probe of 0.56 x 1.3mm front-face dimensions. The distance of the probe from the model

---

[5] *J. R. Ward, F. P. Baltakis, and S. W. Pronchick, "Wind Tunnel Study of Base Drag Reduction by Combustion of Pyrotechnics," ERL Report No. 1745, October 1974. AD# B000431L.*

[6] *F. P. Baltakis, "Wind Tunnel Study of Projectile Base Drag Reduction Through Combustion of Solid, Fuel-Rich Propellants," NOL Wind Tunnel Report No. 93, October 1974.*

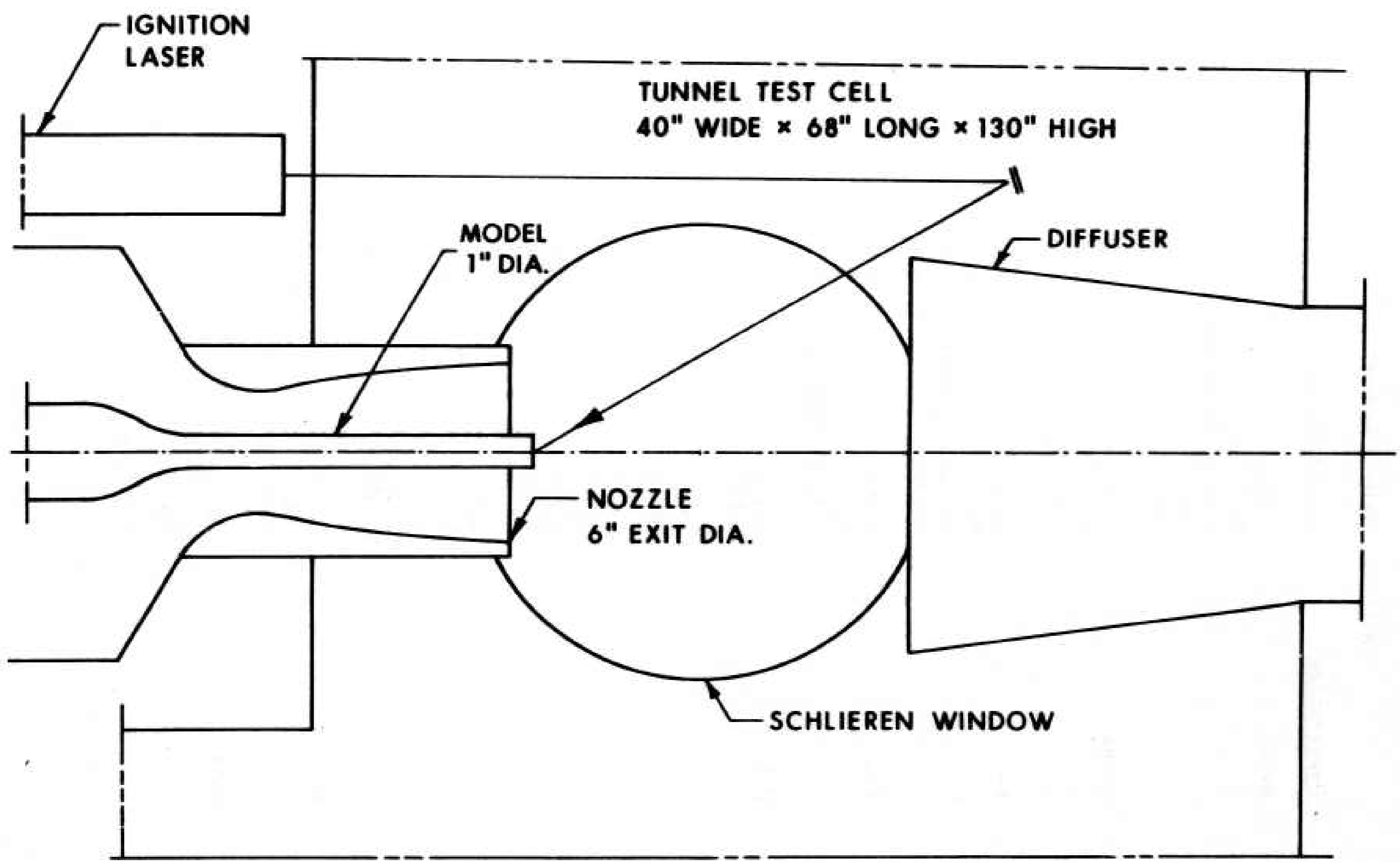

Figure 1. Wind-Tunnel Test Setup

TABLE I. FUMER COMPOSITIONS[a]

Designation	Constituents	
R-20C	SrO_2	65.7
	Mg	21.5
	Calcium Resinate	6.0
	PbO_2	3.4
	BaO_2	3.4
R-284	$Sr(NO_3)_2$	55.0
	Mg	28.0
	Polyvinylchloride	17.0
F-1	SrO_2	78.8
	Mg	8.1
	Calcium Resinate	9.1
	Carbon	4.0
F-4	$Sr(NO_3)_2$	57.7
	Mg	33.2
	Calcium Resinate	9.1
P-1	Coal	97.0
	VAAR[b]	3.0
P-3	MoO_3	57.0
	Ti	43.0
P-5	$NaNO_3$	10.0
	Al	90.0
	VITON A[c]	5.0
	$Mn(CO_3)_2$	2.0
P-7	$NaNO_3$	10.0
	Al	65.0
	C	20.0
	VITON A	5.0
	$Mn(CO_3)_2$	2.0
P-9	NH_4ClO_4	40.0
	Coal	55.0
	VAAR	5.0
P-11	$NaNO_3$	10.0
	Al	85.0
	VITON A	5.0
	$Mn(CO_3)_2$	2.0

TABLE I. FUMER COMPOSITIONS[a]

Continued

Designation	Constituents	
P-13	$NaNO_3$	5.0
	Mg	90.0
	VITON A	5.0
P-15	$NaNO_3$	15.0
	Mg	80.0
	VITON A	5.0
P-17	$NaNO_3$	65.0
	C	35.0
	VAAR	3.0
P-19	$NaNO_3$	15.0
	Al	78.0
	VITON A	5.0
	$Mn(CO_3)_2$	2.0

[a]compositions in percent by weight

[b]vinylalcoholacetate resin

[c]flourinated polymer

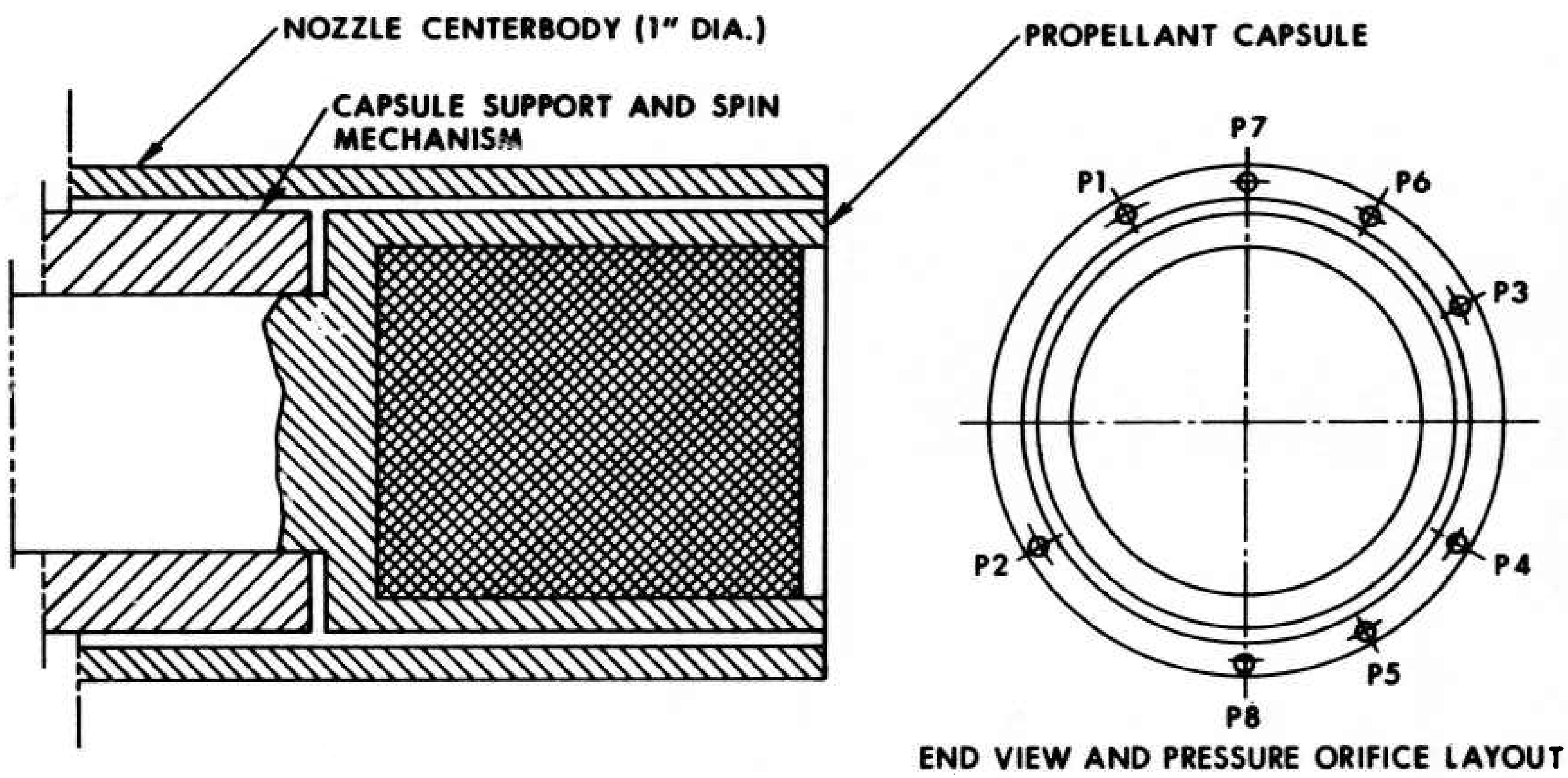

Figure 2. Model Base and Instrumentation Layout

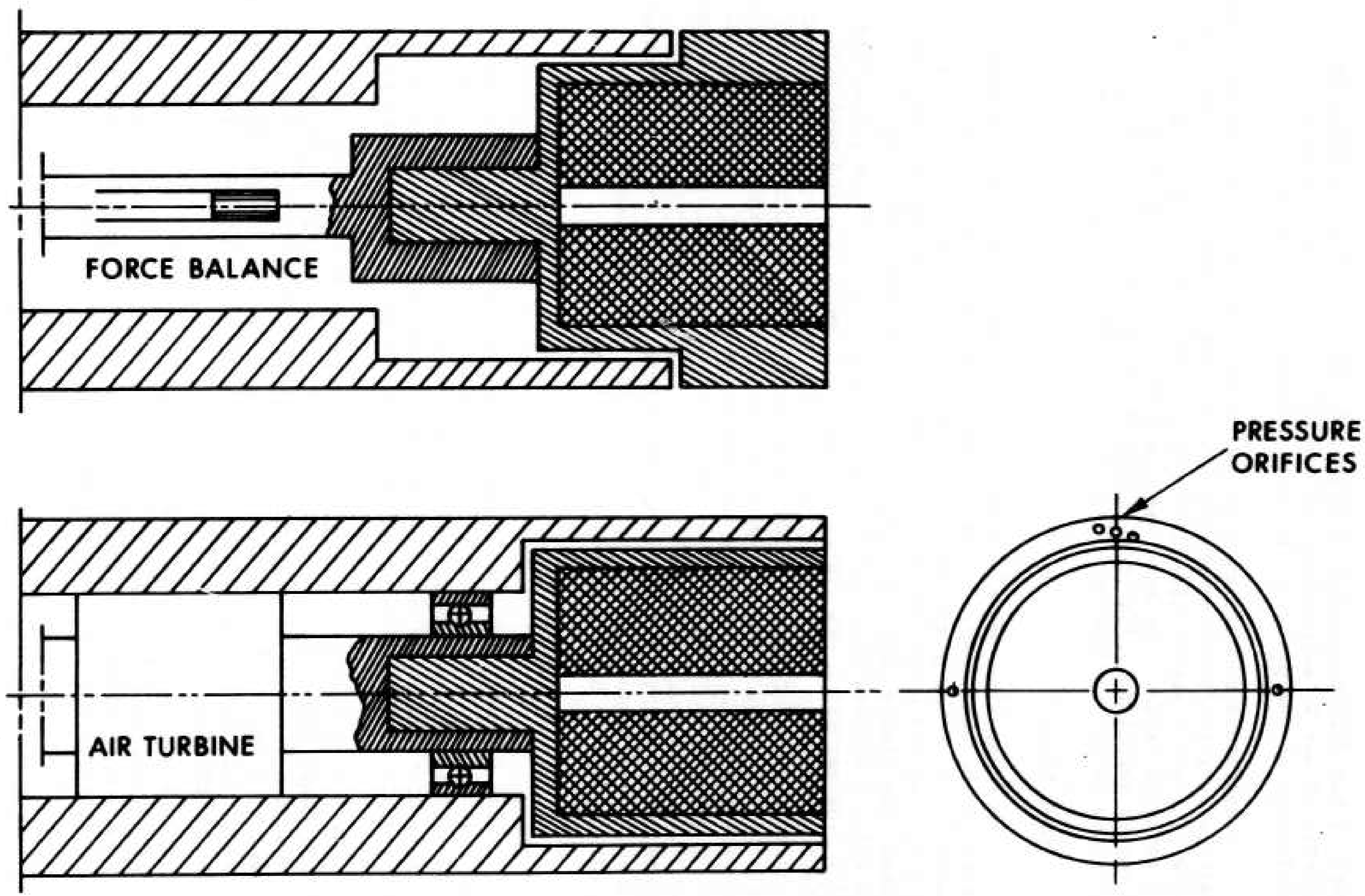

Figure 3. Force Balance and Air Turbine

surface has determined from photographic data in order to avoid inaccuracies due to aerodynamic deflection of the probe. A schlieren photograph of the probe in the flow is shown on Figure 4.

Temperature measurements in the combustion zone were also attempted using a tungsten/tungsten-rhenium thermocouple. The thermocouple was made of 1/4mm diameter wire coated with a very thin layer (1.25×10^{-5}cm) of tantalum oxide. The wire was supported in the stream with a 4mm diameter beryllium oxide rod. Schlieren photographs of the probe in the flow before and during combustion are shown in Figures 5 and 6.

C. Fumer Mixes

The fumer mixes were pressed into the steel capsules mentioned above in the same fashion as described in the first wind tunnel experiments.[5] The fumer mixes were consolidated in the capsules at a pressing pressure of 282 MN/m^2 (40,900 psi). With the exception of R20C, fumer mixes were binary mixes of magnesium and an oxidizer or ternary mixes in which a burning rate modifier was included in the magnesium/oxidizer mix. The magnesium was sieved through a 140 mesh onto 200 mesh screen which corresponds to diameters between 75μ and 100μ. In selected runs a coarser grade of magnesium was used with particle diameters ranging from 150μ to 250μ. The magnesium in the standard pyrotechnic composition, R20C, is grade 12, military specification JAN-M-382(A). Other ingredients conform to specifications stated in reference 7. These ingredients were sieved through a 60 mesh screen. For each fumer mix in the test series, the weight of the mix and the length of the column in the steel capsule were measured. The pyrotechnic mix was designed to be end-burning so as to have a constant mass burning rate.

III. RESULTS

Model boundary layer data are summarized in Figure 7. The measurements were taken at a station 1cm upstream of the model base. At Mach 1.98 additional measurements were taken on the model extension, 14cm further downstream. These data are also included on Figure 7. Different symbols on the plots represent points obtained in different runs.

As may be seen from the graphs, the scatter of the data is small. The boundary layer profile at $M_\infty = 1.98$ flattens out at a slightly lower free-stream Pitot value than the theoretical value. This is presumably caused by a small, local flow disturbance. For the 26.7cm and the 41.9cm models in the Mach 1.98 nozzle, the boundary layer thickness was 2.9mm and 3.6mm respectively.

---

[7] *Engineering Design Handbook, "Military Pyrotechnics Series Part Three - Properties of Materials Used in Pyrotechnic Compositions," AMC Pamphlet 706-187, October 1963.*

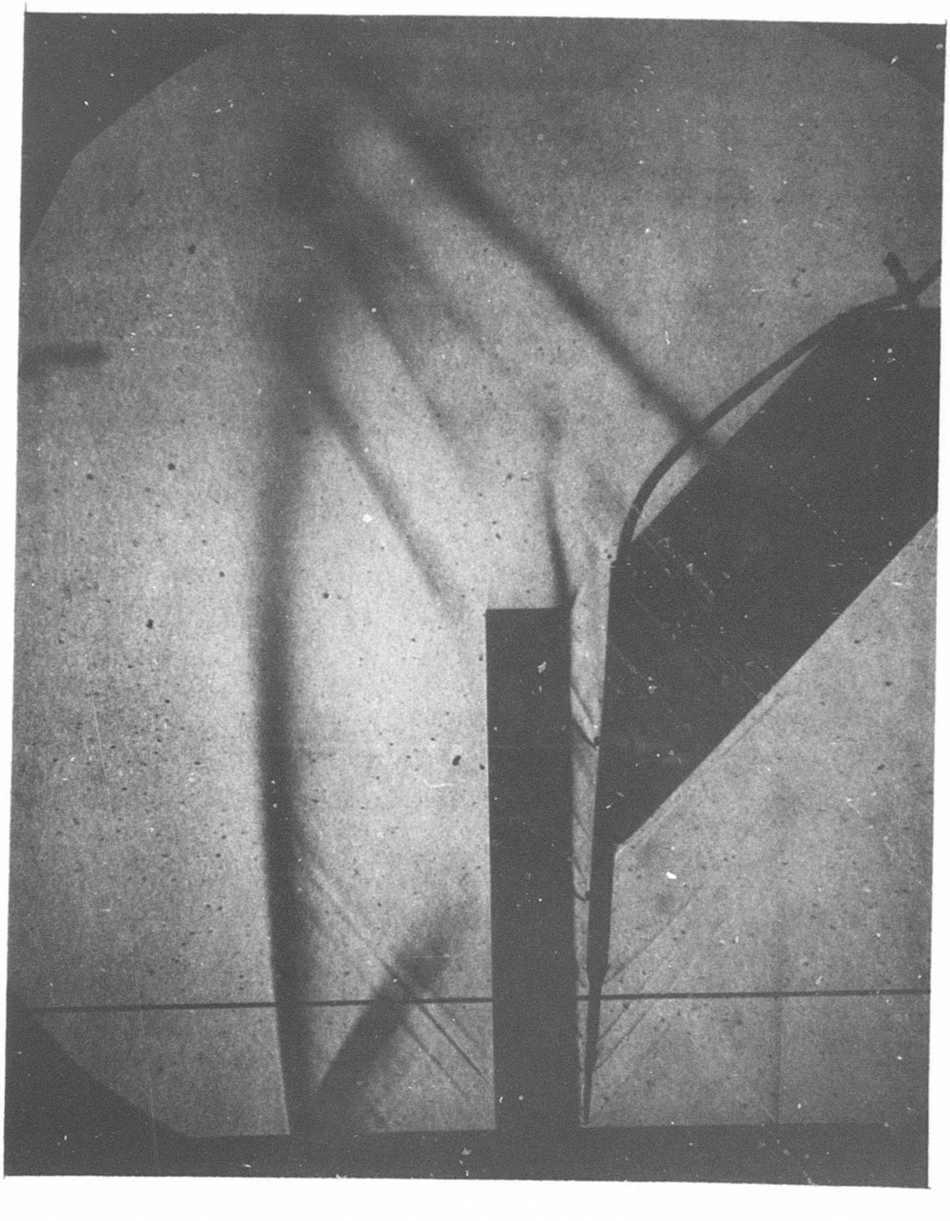

Figure 4. Schlieren Photographs of Flow with Temperature Probe

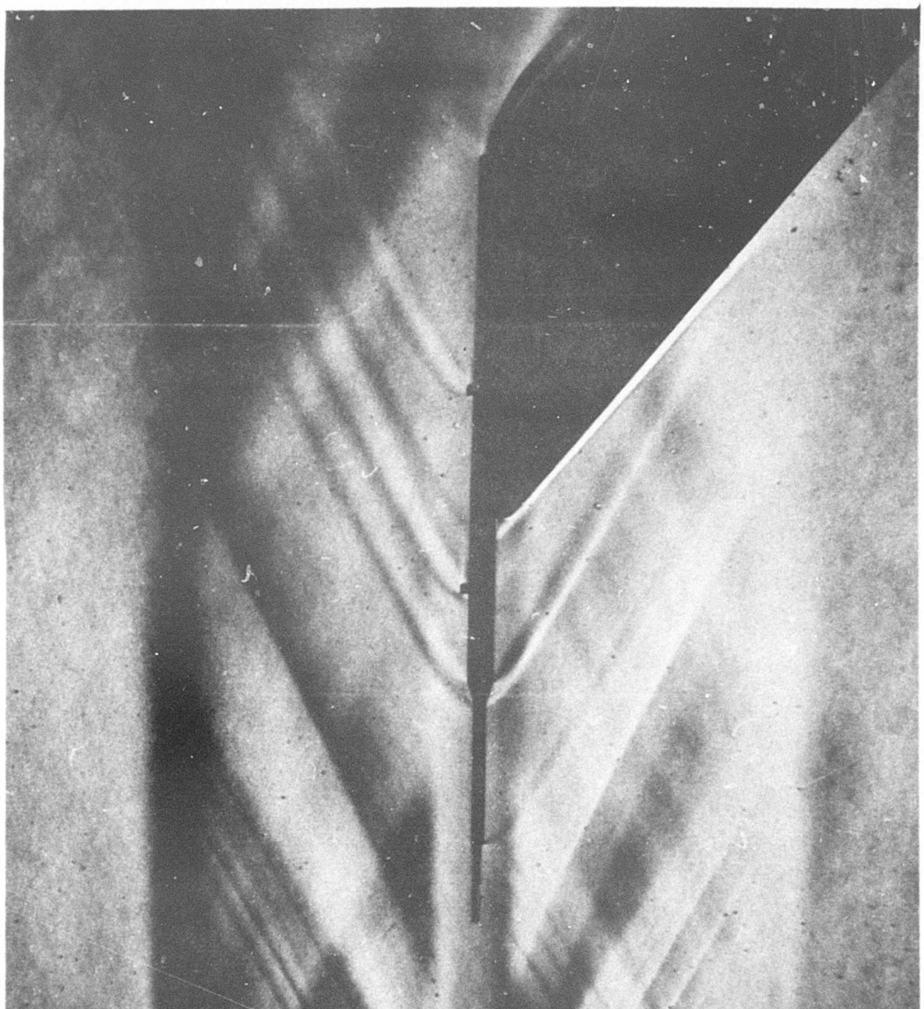

Figure 5. Schlieren Photographs of Flow with Temperature Probe During Combustion, Run 201

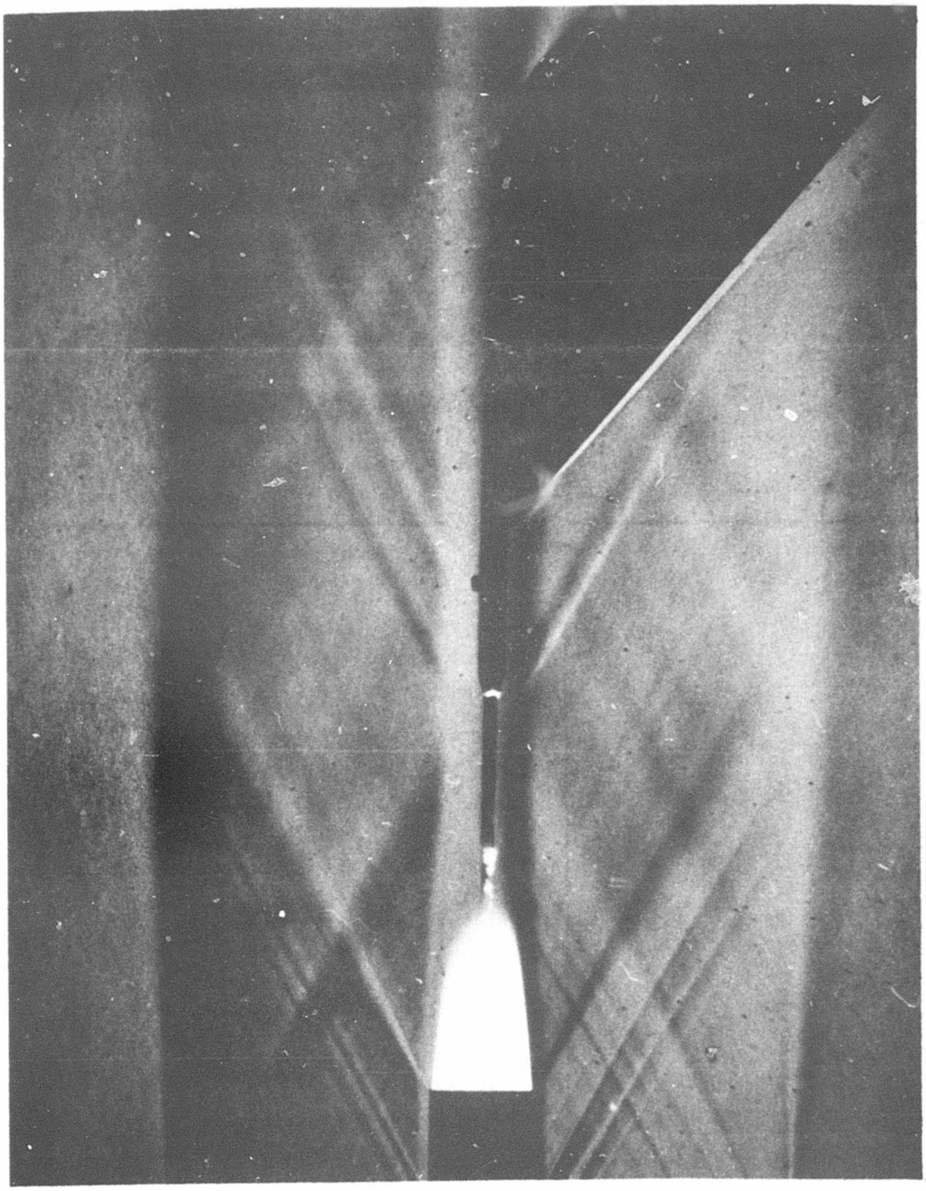

Figure 6. Boundary-Layer Profiles from Pitot Pressure Measurements

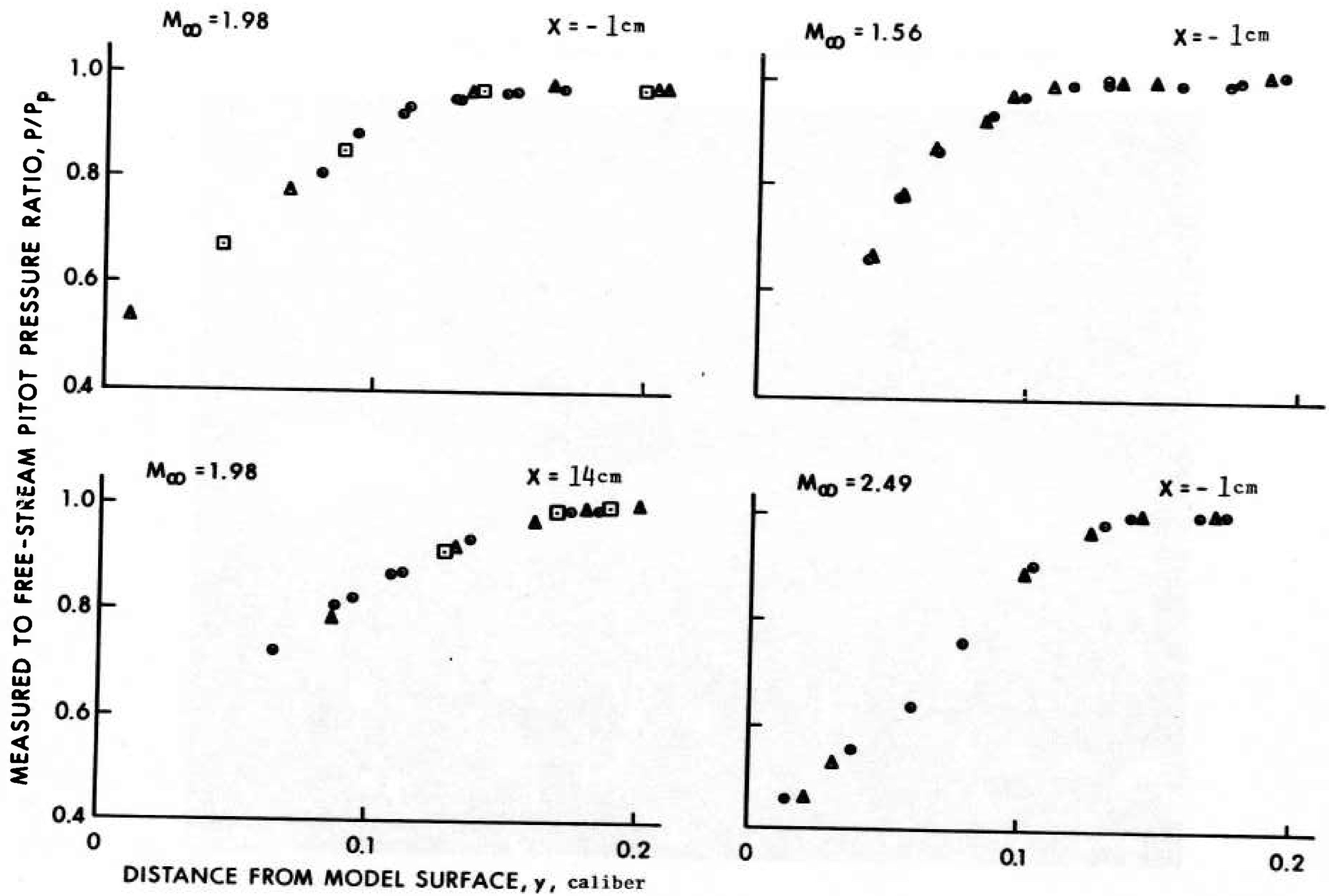

Figure 7. Boundary Layer Profiles From Pitot Pressure Measurements

Temperature measurements in the near-wake were attempted on Runs 201 and 202. On Run 201 the thermocouple was positioned on the wake centerline with the thermocouple junction 5cm downstream of the model base. As combustion of the R20C mix started, the temperature as monitored by the tungsten/tungsten-rhenium thermocouple rose rapidly to about 1900K and remained there within 100K throughout the run. After combustion ceased the measured temperature dropped to 500K. The thermocouple wire was intact although the supporting beryllium oxide rod was badly eroded. On Run 202 a new thermocouple was installed and it was moved two cm closer to the model base. On this run the thermocouple disintegrated as soon as the R20C mix ignited. The thermocouple exceeded the set range of 2800K and no meaningful reading was obtained.

Force balance measurements were attempted in Runs 196 to 202, again utilizing R20C as the fumer mix. Difficulties were experienced first with the balance alignment within the nozzle centerbody, and later with the balance zero shift. The data obtained are not deemed adequate and will be repeated in the next set of wind tunnel tests.

Base pressure variations with time are collected in Appendix B. The pressure is shown normalized to the free-stream static pressure. The base pressure was obtained by averaging readings at two stations (P_1 and P_4). The free-stream static pressure and temperature were computed from the supply pressure and temperature assuming isentropic expansion to Mach 1.98.[8] The Mach number was determined from pre-test nozzle calibrations.

Summaries of the parameters of main interest are presented in Tables II-V. The results were divided this way to facilitate the discussion. The maximum base pressure rise during combustion is self-evident; a median base pressure rise was also estimated from the pressure-time histories, since a slight, but steady increase or decrease in base pressure was frequently observed, e.g., Runs 123 or 132. The burning time of the fumer composition was defined as the interval from the first base pressure rise to the time when the base pressure begins to fall to its pre-combustion value. The mass burning rate is obtained from the mass of the fumer composition divided by the burning time. The injection parameter is defined as follows[9]

$$I = \frac{\dot{m}}{\rho_\infty u_\infty A} \quad . \tag{1}$$

---

[8] *G. P. Sutton, Rocket Propulsion Elements, 3rd ed., John Wiley and Sons, New York, 1963, p. 40.*

[9] *J. E. Bowman and W. A. Clayden, "Reduction of Base Drag by Gas Ejection," RARDE Report 4/69, December 1969.*

Bowman and Clayden[9] contend the injection parameter is the fundamental parameter controlling base pressure rise by gas ejection into the wake. Keyser[10] also correlated base pressure rise with I for wake ejection of cold air at various supersonic velocities. The injection parameter was computed from the following expression that requires terms $\dot{m}$, P_∞, and T_∞ that have already been computed for each run. The injection parameter is

$$I = \frac{\dot{m}}{P_\infty M_\infty A \left(\frac{\gamma M_w}{R T_\infty}\right)^{1/2}} . \tag{2}$$

The density of the fumer mix was computed from the previously measured fumer mass, column length, and the internal diameter of the steel capsule.

IV. DISCUSSION

Table II summarizes results obtained with R20C as the fumer mix. The objectives of these runs were to see the effect of a thicker boundary layer on base pressure rise during combustion and to test the effect of spinning the fumer mix. The latter is important both for simulating projectile flight conditions and also because it presents the opportunity to vary the mass burning rate of fumer mix without changing the chemical composition.[11,12]

The Reynolds numbers for runs with the extended model (Runs 117, 119, 121, and 122) are compared to a run made with the 26.7cm model used in all subsequent tests. The Reynolds number/meter was computed from M_∞, P_o, and T_o.[13] For the extended model, the characteristic length is 41.9cm.

Run	$Re/m \times 10^{-6}$	$Re \times 10^{-6}$
117	53.4	22.4
119	50.0	21.4
121	48.7	20.4
122	48.7	20.4
124	51.7	13.8

[10] *L. D. Keyser, "Effects of Base Bleed and Supersonic Nozzle Injection on Base Pressure," BRL Memorandum Report No. 2456, March 1975. AD# B003442L.*

[11] *J. J. Caven and T. Stevenson, "Pyrotechnics for Small Arms Ammunition," Frankford Arsenal Report R-1968, July 1970.*

[12] *W. Puchalski, "The Effect of Angular Velocity and Composition on Pyrotechnic Performance," Frankford Arsenal Technical Report 74011, August 1974.*

[13] *D. J. Spring and K. L. Blackwell," Tables for Calculation of Reynolds Number as a Function of Mach Number, Stagnation Pressure, and Stagnation Temperature," US Army Missile Command Report RD-TR-63-3, February 1963.*

TABLE II

Wind Tunnel Runs With R20C

Run No.	T_∞,K	P_∞,bar	------(Pb/P∞)------- int.	max.	med.	tb,sec	m,g	ρ,g/cm^3	$\dot{m}$,g/sec	I x 10^3	spin,krpm
117[a]	261	1.04	0.65	0.87	0.86	2.7	9.8	2.59	3.6	8.0	---
119[a]	280	1.09	.64	.84	.83	3.3	10.1	2.50	3.1	6.7	---
121[a]	290	1.09	.63	.84	.83	3.1	11.4	2.60	3.7	8.2	---
122[a]	291	1.10	.60	.84	.82	3.0	10.3	2.55	3.4	7.5	---
124	279	1.11	.63	.83	.82	2.6	10.5	2.54	4.0	8.7	---
153	279	1.06	.63	.87	.87	.98	10.2	2.54	10	23	35
154	285	1.07	.62	.86	.86	1.0	10.6	2.54	11	24	11
155	283	1.06	.63	.87	.86	.89	10.5	2.49	12	27	30
162	289	1.04	.62	.86	.86	1.0	9.8	2.52	9.8	22	13
164	294	1.03	.62	.87	.86	.92	10.3	2.54	11	27	45
189	273	1.06	.64	.89	.89	.97	11.4	2.53	12	26	45
190	269	1.04	.64	.89	.89	.88	10.8	2.51	12	28	52

[a]Extended wind tunnel model.

TABLE III

Wind Tunnel Runs with Binary Mg-SrO_2 Mixes

Run No.	T_∞,K	P_∞,bar	----(P_b/P_∞) int.	max.	med. --------	tb,sec	m.g	ρ,g/cm^3	$\dot{m}$,g/sec	I x 10^3
126	282	1.09	0.62	0.74	0.70	6.0	11.8	2.93	2.0	4.4
127	277	1.09	.61	.78	.78	2.0	11.7	2.82	5.8	13
128	276	1.09	c	.86	.85	1.4	10.4	2.67	7.4	16
132	274	1.07	.61	.87	.86	1.1	10.3	2.54	9.4	21
134	276	1.07	.61	.74	.70	5.2	11.2	2.68	2.5	4.8
137[a]	277	1.05	.61	.78	c	c	10.5	c	---	---
138[b]	279	1.05	.62	.77	c	c	10.7	2.80	---	---

[a]Center-perforated tungsten washer to reduce burning surface by 50%

[b]Center-perforated tungsten washer to reduce burning surface by 75%

[c]Not measured

TABLE IV

Wind Tunnel Runs With Calcium Resinate
Added to 15/85 Mg-SrO_2 Mix

Run No.	T_∞,K	P_∞ bar	(Pb/P_∞) int.	(Pb/P_∞) max.	(Pb/P_∞) med.	tb,sec	m,g	ρ,g/cm^3	$\dot{m}$,g/sec	I x 10^3
126	282	1.09	0.62	0.74	0.70	6.0	11.8	2.93	2.0	4.4
139	281	1.06	.61	.72	.70	5.0	11.0	2.84	2.2	5.0
140	280	1.06	.61	.74	.73	4.2	11.1	2.77	2.6	6.0
141	280	1.05	.62	.79	b	3.1	10.5	2.73	3.4	7.7
142	279	1.06	.61	.78	b	4.1	10.7	2.69	2.6	5.9
143	279	1.05	.61	.78	b	4.8	10.2	2.58	2.1	4.8
144	278	1.08	.61	.77	b	5.5	10.5	2.39	1.9	4.2
192[a]	270	1.06	.62	.82	.81	2.8	12.5	3.12	4.5	10
193[a]	271	1.06	.63	.80	.79	2.9	11.0	2.79	3.8	8.4

[a] BaO_2 as oxidizer

[b] Not determined

TABLE V

Wind Tunnel Runs With Addition of Other Burning Rate Modifiers

Run No.	T_∞,K	P_∞,bar	(Pb/P_∞) int.	(Pb/P_∞) max.	(Pb/P_∞) med.	tb,sec	m,g	ρ,g/cm^3	$\dot{m}$g/sec	I x 10^3
147	276	1.06	0.61	0.70	0.70	5.6	10.9	2.80	2.0	4.4
148	276	1.08	.61	.73	.73	3.9	10.7	2.66	2.7	6.0
149	275	1.07	.61	.76	.74	3.6	10.3	2.50	2.9	6.3
166	296	1.09	.62	.70	.68	6.7	11.4	2.74	1.7	3.8
150	275	1.08	.61	.71	.71	7.0	10.5	2.51	1.5	3.3
151	276	1.09	.61	.71	.70	9.8	10.5	2.45	1.1	2.3
167	297	1.11	.62	.71	.71	6.4	11.0	2.83	1.7	3.8
168	295	1.10	.61	.71	.71	6.8	10.5	2.59	1.5	3.3
169	294	1.11	.61	.73	.71	8.1	10.5	2.48	1.4	2.8

A comparison between runs made with the two models is presented below. R20C was the fumer mix in these runs.

Run	Re x 10^{-6}	$\Delta(P_b/P_\infty)$	$\dot{m}$, g/s	I x 10^3
117[a]	22.4	0.21	3.6	8.0
119	21.4	0.19	3.1	6.7
121	20.4	0.20	3.7	8.2
122	20.4	0.22	3.4	7.5
124[b]	13.8	0.19	4.0	8.7

[a] δ/d = 0.14 for extended length model

[b] δ/d = 0.12 for normal length model

These results suggest that the variation in Reynolds number and boundary layer thickness do not markedly change the base pressure rise. From a projectile design standpoint, it means the results in the wind tunnel with a model of length-to-diameter ratio of 10.5 are comparable with base pressure changes in projectiles which have ℓ/d-ratios from 3-5.5.[1] These results are also consistent with those of Bowman and Clayden[9] who performed similar experiments with gases ejected into the wake.

These set of runs also illustrate the variation in burning rate for pyrotechnic mixes. The burning rate of R20C varied from 3.1 to 4.0 g/s. Similar variations were observed in pyrotechnic strand burning rate measurements at high external pressures.[14] The burning rate in these experiments was measured directly from high-speed films of the burning pyrotechnic as opposed to the indirect estimate of burning time made in the wind tunnel tests. It was noted during the linear burning rate measurements that the burning rate variation decreased at the higher pressures.

The results for R20C at varying spin rates are summarized in Figures 8 and 9 in which mass burning rate vs spin rate and $\Delta(P_b/P_\infty)$ vs the injection parameter, I, are plotted.

---

[14] *L. Decker and J. R. Ward, "Linear Burning Rates of Pressed Propellants," BRL Memorandum Report in press.*

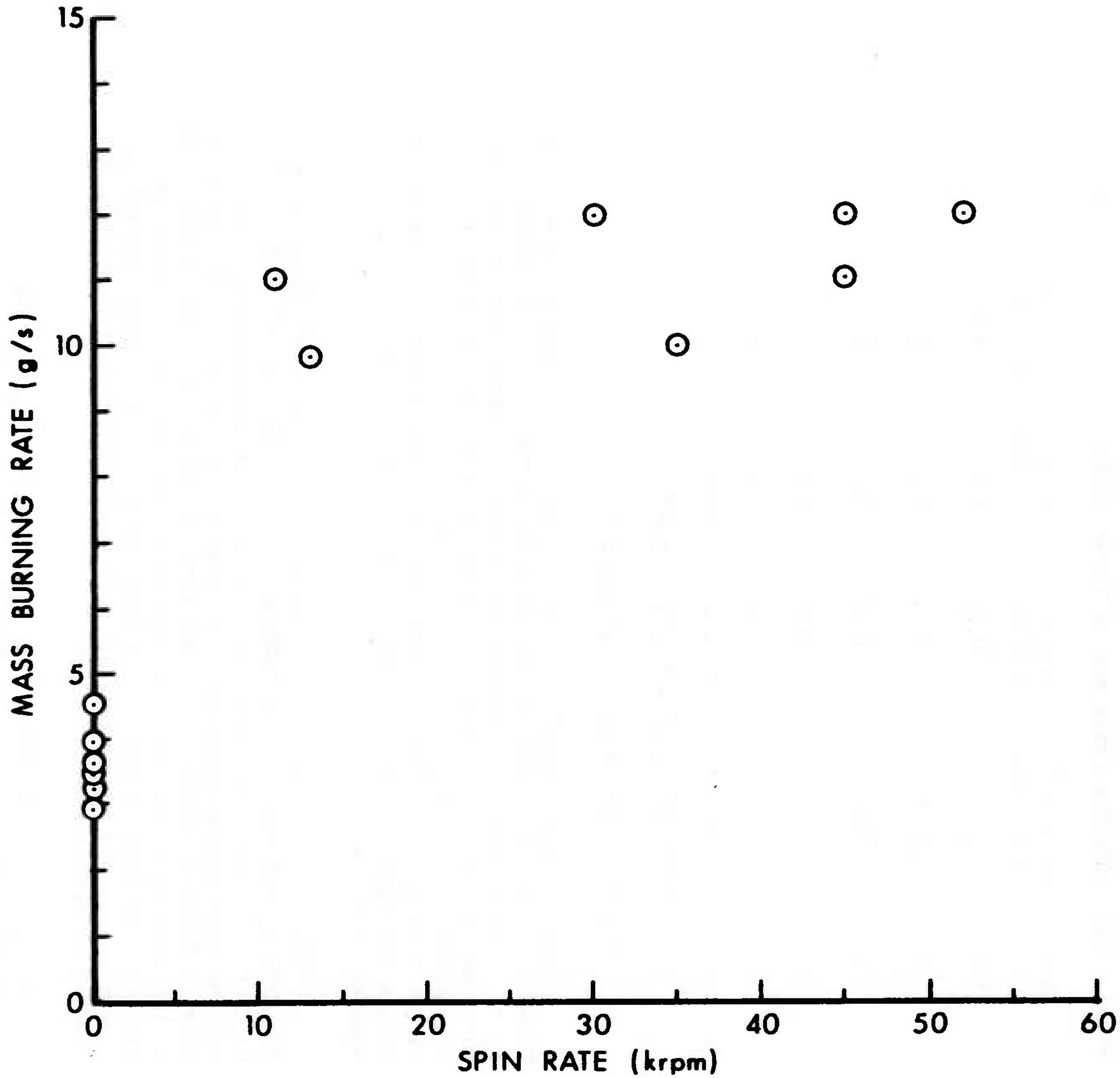

Figure 8. Mass Burning Rate of R20C vs Spin Rate

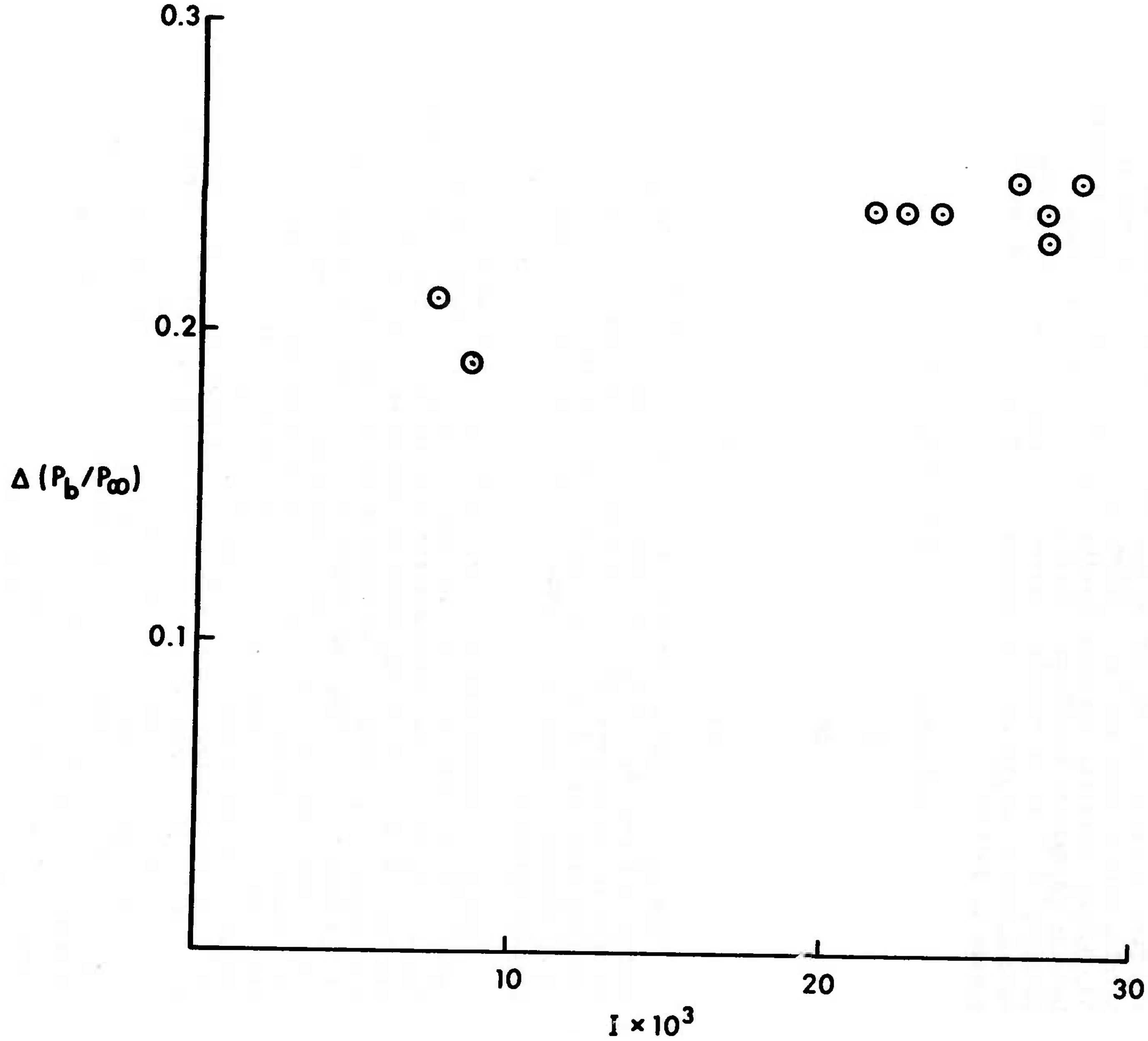

Figure 9. Change in Base Pressure Rate _vs_ Injection Parameter for R20C

The first point to be noticed is that the spin increases the mass burning rate of R20C from an average value of 3.5 g/s to 12 g/s at 52,000rpm. However, the mass burning rate is not changed dramatically between 10,000 and 52,000rpm. This is in accord with previous results.[11,12] For a 36.3/63.7 percent by weight binary mix of magnesium/strontium nitrate, the burning rate *versus* spin rate was reported as follows[12]

Spin, krpm	Burn rate, cm/s
20	0.41
28	0.41
35	0.46
43	0.48

The second point of interest is the trend of $\Delta(P_b/P_\infty)$ *vs* I depicted in Figure 8. It appears there is a limit to the base drag reduction as the burning rate of the fumer mix increases. Similar conclusions were reached in other wind tunnel experiments[9,10,15] in which nitrogen, argon, or air were injected into the wake region at various values of I.

Table III summarizes data testing the influence of the fuel content, fuel particle size, and the addition of center-perforated tungsten washers. The rationale for testing fuel content came from a previous report[16] that suggested the base-drag reducing capability of a pyrotechnic mix would be enhanced by making the fumer mix fuel-rich. It was hypothesized that the excess fuel would vaporize and subsequently burn in the wake region. In the first wind tunnel series[5], the fuel-rich magnesium/strontium nitrate mixes could not be ignited. In this test series, strontium peroxide was substituted for strontium nitrate. On the assumption that Mg/SrO_2 will react to form MgO and SrO, then the stoichiometric mix of Mg/SrO_2 will contain 17% by weight magnesium. The particle size of the magnesium was varied to provide a test of chemically identical fumer mixes with different burning rates. The center-perforated washers were used to test the effect of varying the diameter of the fumer cavity as was done by Reid and Hastings[15] (Figure 10) and more recently by Keyser[10]. In the first wind tunnel series,

---

[15] *J. Reid and R. C. Hastings, "The Effect of a Central Jet on the Base Pressure of a Cylindrical Afterbody in a Supersonic Stream," RAE Report No. Aero. 2621, December 1959.*

[16] *J. R. Ward and R. K. Pahel, "Fuel-Rich Magnesium/Oxidizer Mixes as Drag-Reducing Fumers," BRL Memorandum Report No. 2336, October 1973. AD# 771171.*

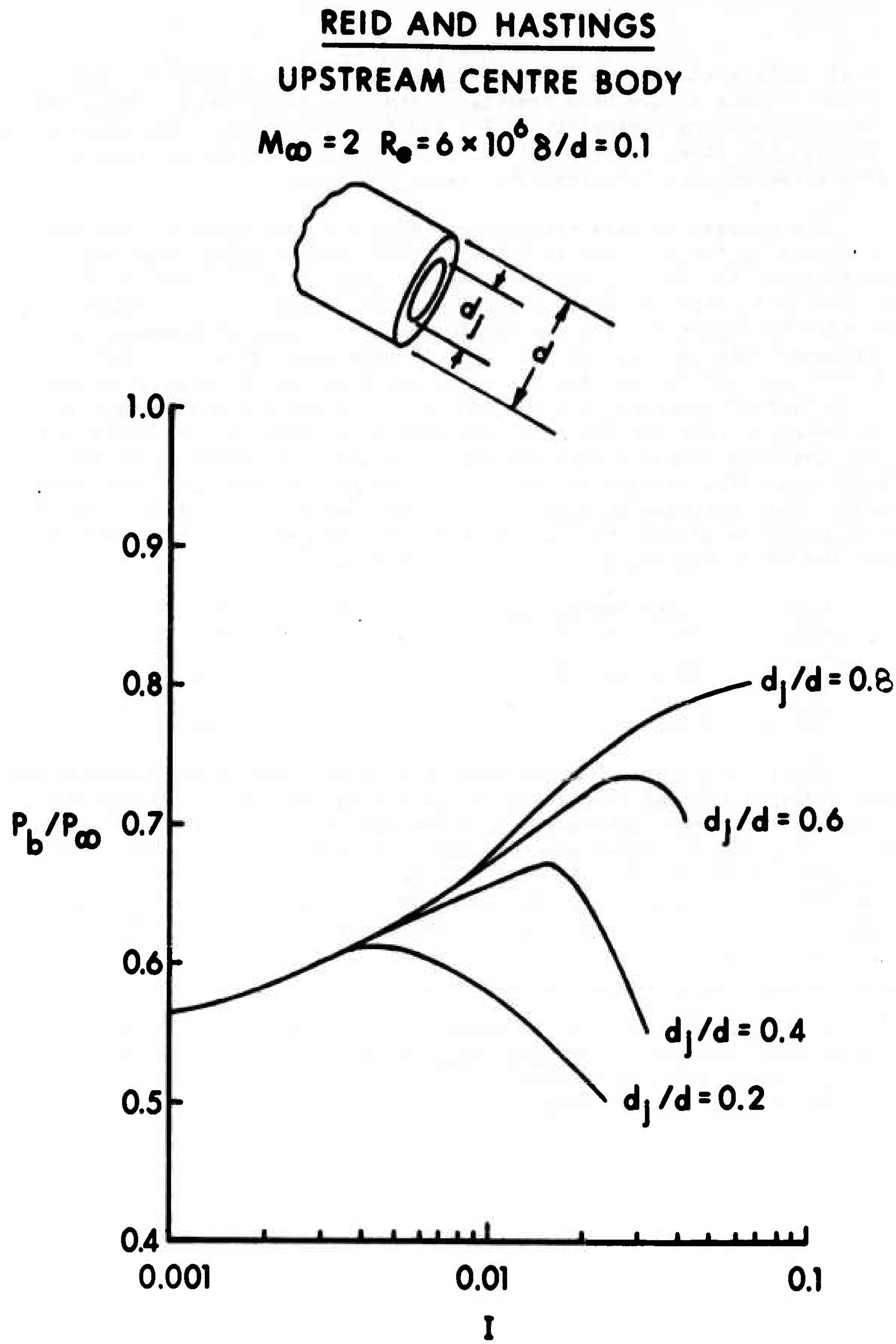

Figure 10. Change in Base Pressure Ratio vs I for Different Various Fumer Cavity Diameters

steel washers similar to those employed in 7.62[4] and 20mm[17] firings melted. Since it has been reported[18] that the steel washers improved the drag-reducing capability of F-4 and that recovered 7.62mm projectiles revealed the steel washers did not melt, the tests with the washers were repeated with tungsten substituted for steel.

The changes in base pressure vs injection parameter are plotted in Figure 11 for the runs in Table III for which burning times were available. The first point to notice is that the base pressure increase is directly related to the injection parameter in a fashion similar to Figure 8. The results for the coarse-grade magnesium mix are especially interesting, since the coarse-grade fuel-rich 20/80 Mg/SrO_2 has nearly the same injection parameter as the regular grade, nearly stoichiometric, 15/85 Mg/SrO_2 mix. On the assumption made in reference 16 that the fuel-rich mix should be superior, one would expect the base pressure rise for the 20/80 mix to be higher than the 15/85 mix. The results in Table III (compare 126 with 134) contradict this, since the base pressure rise is the same for both mixes. The same conclusion is evident from a comparison between spinning R20C (Run 162) and the 30/70 Mg/SrO_2 Run (132) as shown below

Run	Fumer Composition	$\Delta(P_b/P_\infty)$	I
132	30/70 Mg/SrO_2	0.25	0.021
162	R20C	0.24	0.022

The interpretation of the results with the washers was hampered by not having a burning time available (see Runs 136 and 137 in Appendix B). However, the base pressure rise was the same as the run with no washer (Run 127), and the fumer specific impulses were nearly identical (1280 and 1240 N-s/kg for Runs 127 and 137, respectively). For this to be so and with the pressure rise the same, the burning times had to be the same. Thus, the center-perforated washers did not seem to influence fumer performance.

---

[17] *T. A. Elmendorf and R. A. Trifiletti, "Gas Generators for Base Drag Reduction (Fumers)," Aerodynamics of Base Combustion, S. N. B. Murthy et al, eds., HIT Press, Boston, in press.*

[18] *R. Kwatnoski, private communication.*

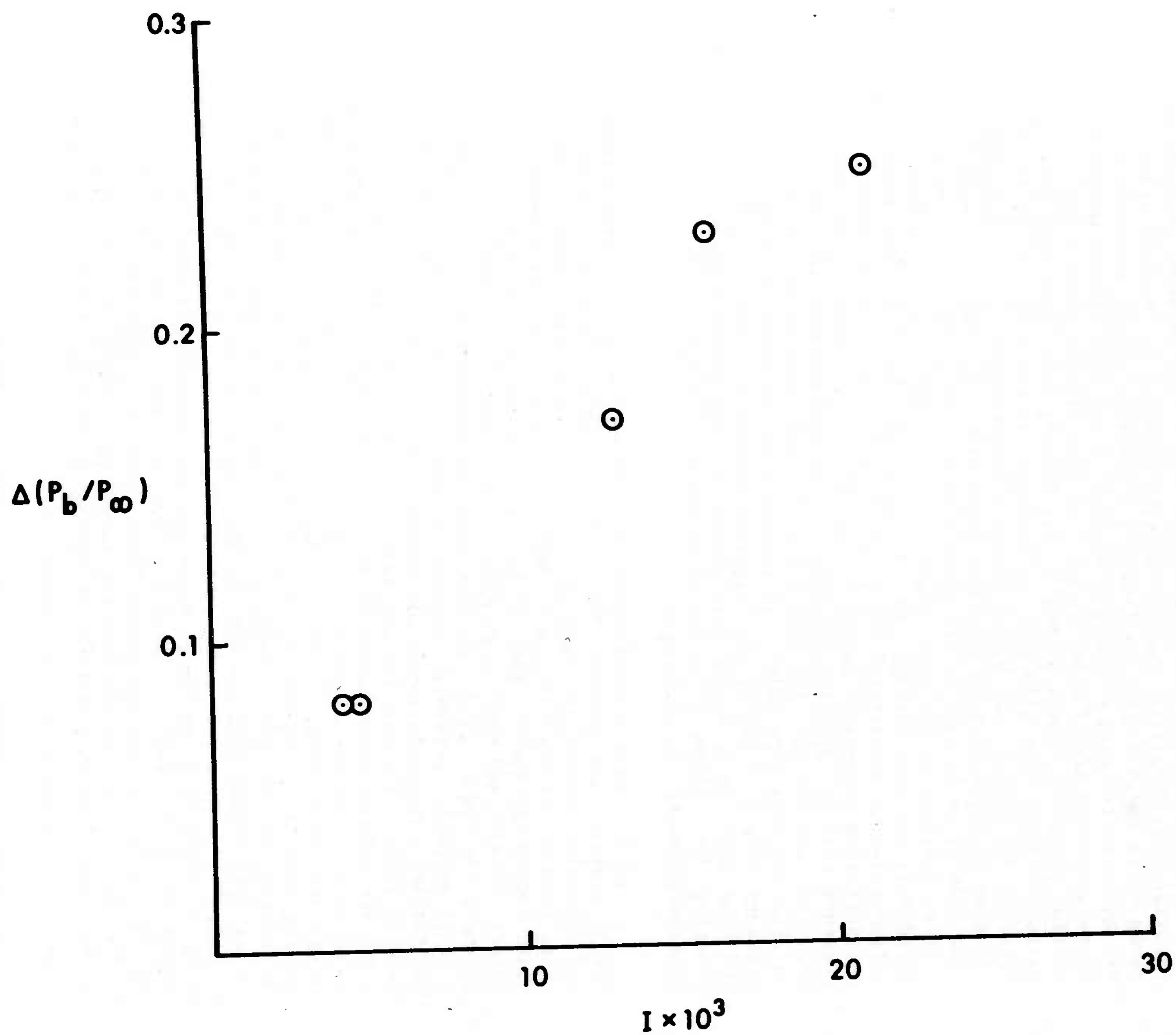

Figure 11. Change in Base Pressure Ratio vs Injection Parameter for Binary Mg-SrO_2 Mixes

Table IV summarizes data for a series of runs in which varying amounts of calcium resinate were added to a binary magnesium/strontium peroxide mix. Additives such as calcium resinate are used in pyrotechnics to improve the consolidation properties of the pyrotechnic mix and are also used as color intensifiers and burning rate modifiers. These additives are of interest because they produce gaseous combustion products as well as modify the burning rate. The pressure-time plots for these runs (139-144) did not exhibit the step-like plots as obtained for R20C or the binary mixes of magnesium/strontium peroxide. The type of pressure-time plot for these runs is presumably caused by slag forming on the lip of the model rather than anomalies in the combustion behavior of the mix. Median base pressure rises were estimated only for runs 139 and 140. Two runs (192-193) were made with barium peroxide substituted for strontium peroxide. The resulting pressure-time plots were easier to interpret. In Figure 12 the base pressure rise <u>vs</u> injection parameter is plotted for runs 139, 140, 192, 193, and run 126, the binary mix to which varying amounts of calcium resinate were added. It appears that the trend of base pressure rise with increasing injection parameter is still followed, and that there is no discernible effect of fumer performance by changing the oxidizer or by adding an additive except to vary the injection parameter by changing $\dot{m}$.

In Table V data are collected for runs made with polyvinylchloride (PVC), oxamide, and gelatin. PVC is used in pyrotechnics as a binder and red-color intensifier in tracer mixes. Oxamide was chosen, since it is used as a flame-retardant[18] and it was hoped that the oxamide would reduce the burning rate of fast-burning fuel-rich pyrotechnic mixes. Gelatin was used as an additive in 7.62mm[4] and 20mm[17] firings. In Figure 13 one can see that the general trend of base pressure rise <u>vs</u> injection parameter observed in previous runs is again followed, but further interpretation is difficult because of uncertainties in the burning times. The mass burning rates and linear burning rates for these mixes are summarized in Tables VI and VII. The linear burning rate is estimated by dividing the length of the fumer mix by the burning time. Two things are interesting. First, the addition of oxamide increases the burning rate of the Mg/SrO_2 mix rather than decrease it as anticipated. Apparently, the oxamide is reacting with magnesium or strontium peroxide rather than decomposing and cooling the surface of the burning pyrotechnic.[19] Oxamide does reduce the burning rate of a standard 20mm tracer which is composed primarily of magnesium and strontium nitrate. The second point of interest is that addition of gelatin or PVC has about the same effect on burning rates. Gelatin has been proposed as a particularly effective additive for fumer application,[4] but the wind tunnel results suggest that PVC is just as effective. PVC has the added

---

[19] *I. W. Lyons, <u>The Chemistry and Use of Fire Retardants</u>, Wiley-Interscience, 1970, pp 14-22.*

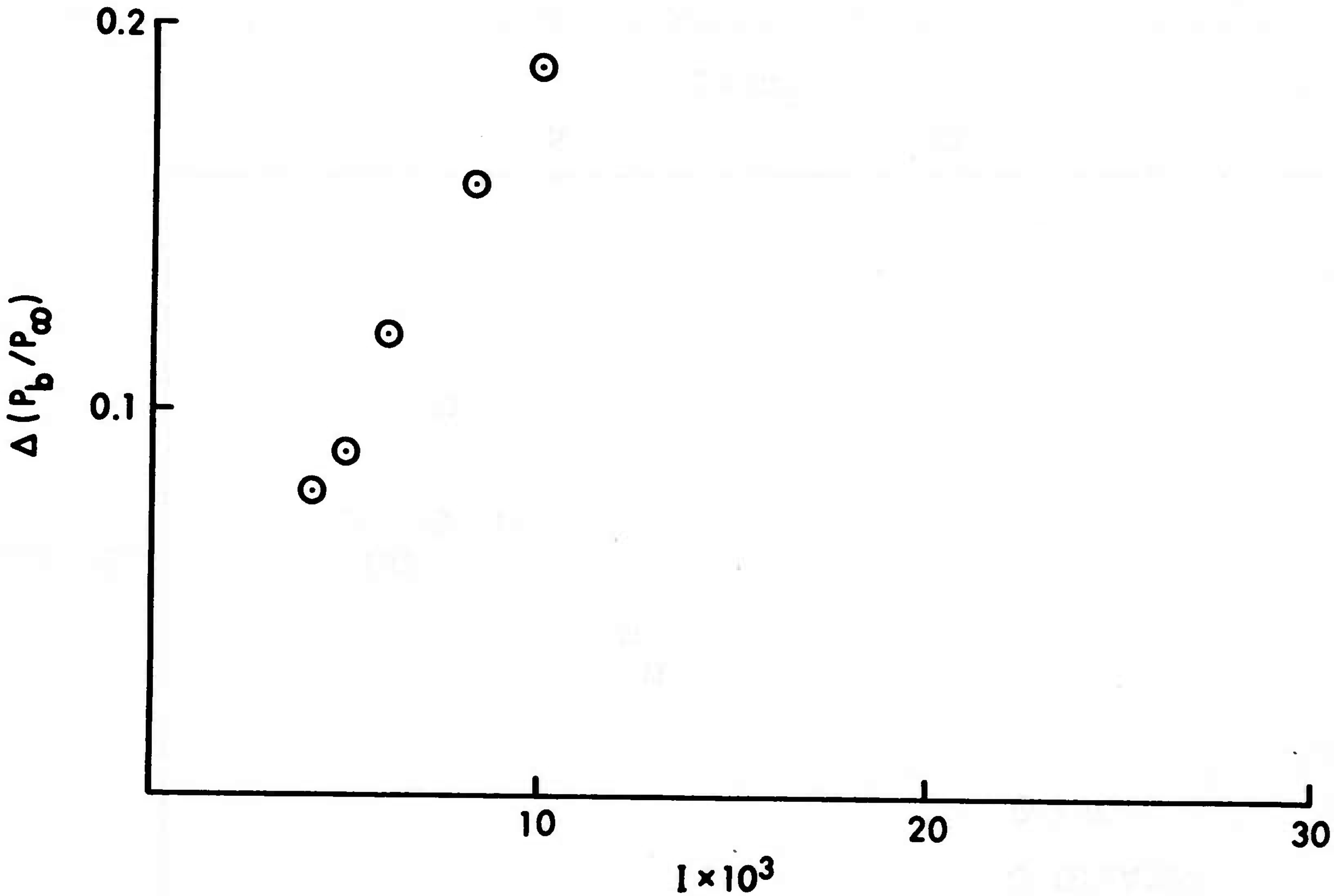

Figure 12. Change in Base Pressure Ratio _vs_ Injection Parameter for Calcium Resinate Added to $Mg-SrO_2$ and $Mg-BaO_2$ Mixes

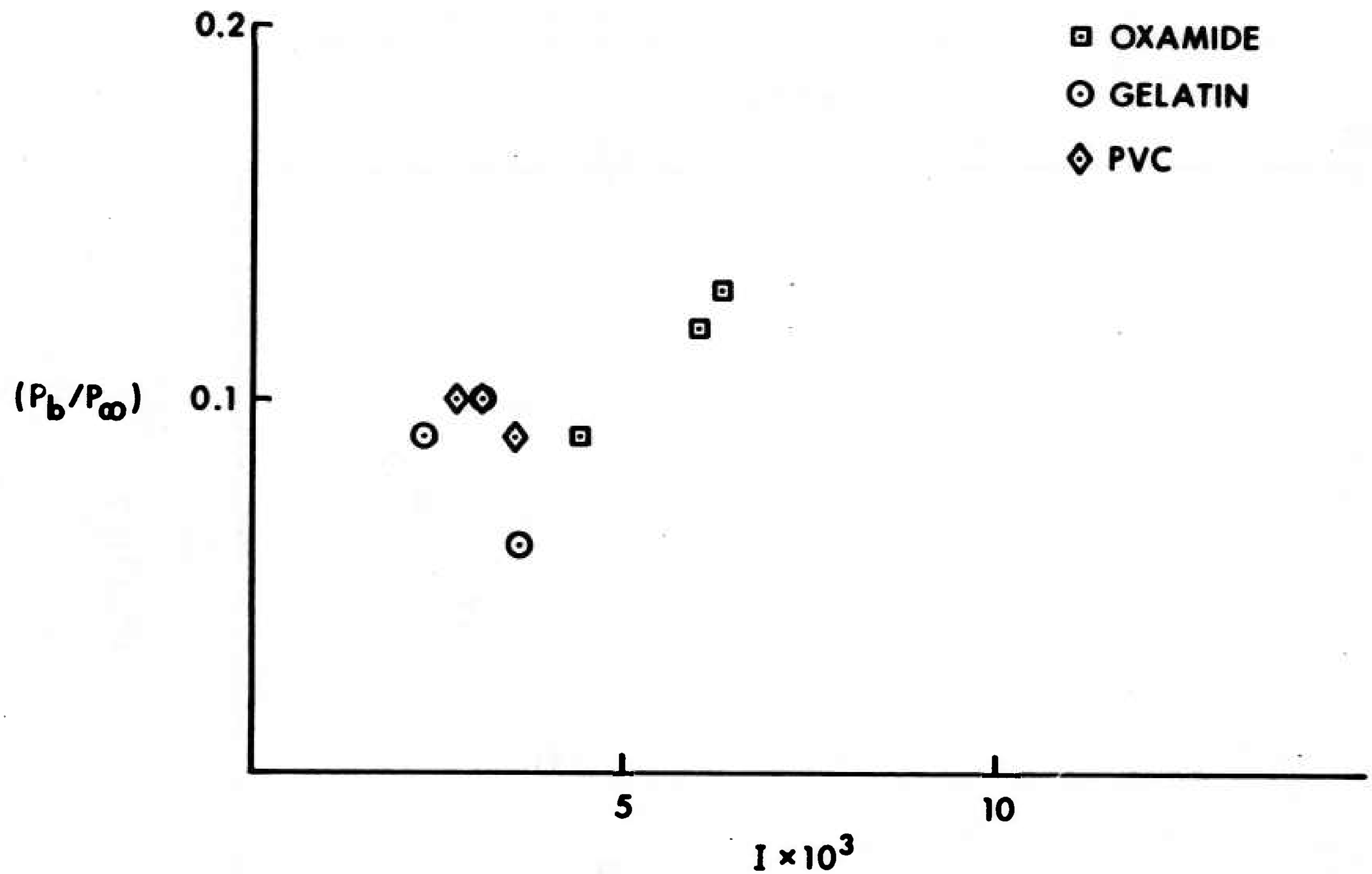

Figure 13. Change in Base Pressure Ratio for Different Binders Added to a 15/85 Mg-SrO_2 Mix

TABLE VI

Comparison of the Effect of Various Pyrotechnic Binders on Mass Burning Rate

Fumer[a]	Mass Burning Rate, g/sec				
	CR[b]	PVC[c]	OX[d]	GEL[e]	NONE
15Mg 85SrO$_2$	---	---	---	---	2.0
14Mg 81SrO$_2$ 5 binder	3[f]	1.7	2.0	1.7	---
14Mg 76SrO$_2$ 10 binder	2.1	1.5	2.7	1.5	---
13Mg 72SrO$_2$ 15 binder	1.9	1.4	2.9	1.1	---

[a] fumer composition in percent by weight

[b] calcium resinate

[c] polyvinylchloride

[d] oxamide

[e] gelatin

[f] interpolated from mass burning rates of 4 and 6% CR.

TABLE VII

Comparison of the Effect of Various Pyrotechnic Binders on Linear Burning Rate

Fumer[a]	Linear Burning Rate, cm/sec				
	CR[b]	PVC[c]	OX[d]	GEL[e]	NONE
15Mg $85SrO_2$					0.30
14Mg $81SrO_2$ 5 binder	0.48[f]	0.27	0.30	0.28	---
14Mg $76SrO_2$ 10 binder	.35	.26	.45	0.26	---
13Mg $72SrO_2$ 15 binder	.36	.23	.50	0.19	---

[a] Fumer composition in percent by weight

[b] calcium resinate

[c] polyvinylchloride

[d] oxamide

[e] gelatin

[f] interpolated from linear burning rates of 4 and 6% CR.

advantage of increasing the red color value of tracer mixes[20] which would be an important consideration if fumer mixes will also have to be used as tracer mixes.

In Figure 14 all the previous runs are replotted on a single graph. In Figure 15 these runs are plotted as base drag coefficient vs injection parameter. The base pressure ratio, P_b/P_∞, is related to the base drag coefficient by

$$C_{Db} = \frac{1 - (P_b/P_\infty)}{1/2\ \gamma M_\infty^{\ 2}} \quad . \tag{4}$$

The trend of decreasing base drag coefficient with increasing I is evident. Bowman and Clayden[9] expressed this trend as

$$C_{Db} = CD_{b_o}\ e^{-J \times I} \quad . \tag{5}$$

The parameter J was found to be a function of Mach number, temperature, and the molecular weight of the injected gas. Bowman and Clayden estimated what the parameter J in Eq. (5) would be for injection of a propellant gas with molecular weight of 18 g/mole and temperature of 2500K. The base drag coefficient vs I for Bowman and Clayden's hypothetical propellant is also plotted on Figure 15 which shows that the base drag reduction for a given injection parameter is comparable to that for the pyrotechnics. It remains to be seen whether Bowman and Clayden's estimates for a propellant are realistic. Nonetheless, this raises the possibility of "invisible" fumers. Shidlovskii[21] states that solid propellant combustion gases do not emit sufficient luminous energy to be of use as tracers. On the other hand, Puchalski[22] has contended it is not possible to design a non-luminous fumer formulated with pyrotechnics.

The analysis of data has been concerned with Mg/SrO_2 mixes at a single Mach number. In the previous report,[5] some runs were performed with strontium nitrate as the oxidizer and some runs were made at Mach numbers of 2.49 and 1.56. The median base pressure rises, burning times, and injection parameters for these earlier runs are given in Table VIII. A plot of base-pressure use vs I for these runs is given in Figure 16.

---

[20] *D. Hart and H. J. Eppig, "Long Range Research on Pyrotechnics: Burning Characteristics of Binary Mixes," Picatinny Arsenal Technical Report 1669, October 1947.*

[21] *A. A. Shidlovskii, Bases of Pyrotechnics, in Russian, 1964, translated version available as Picatinny Arsenal Technical Memorandum 1615, May 1965.*

[22] *W. J. Puchalski, "An Analysis to Determine the Feasibility of a Non-Luminous Pyrotechnic Fumer," Frankford Arsenal Technical Report-74036, December 1974.*

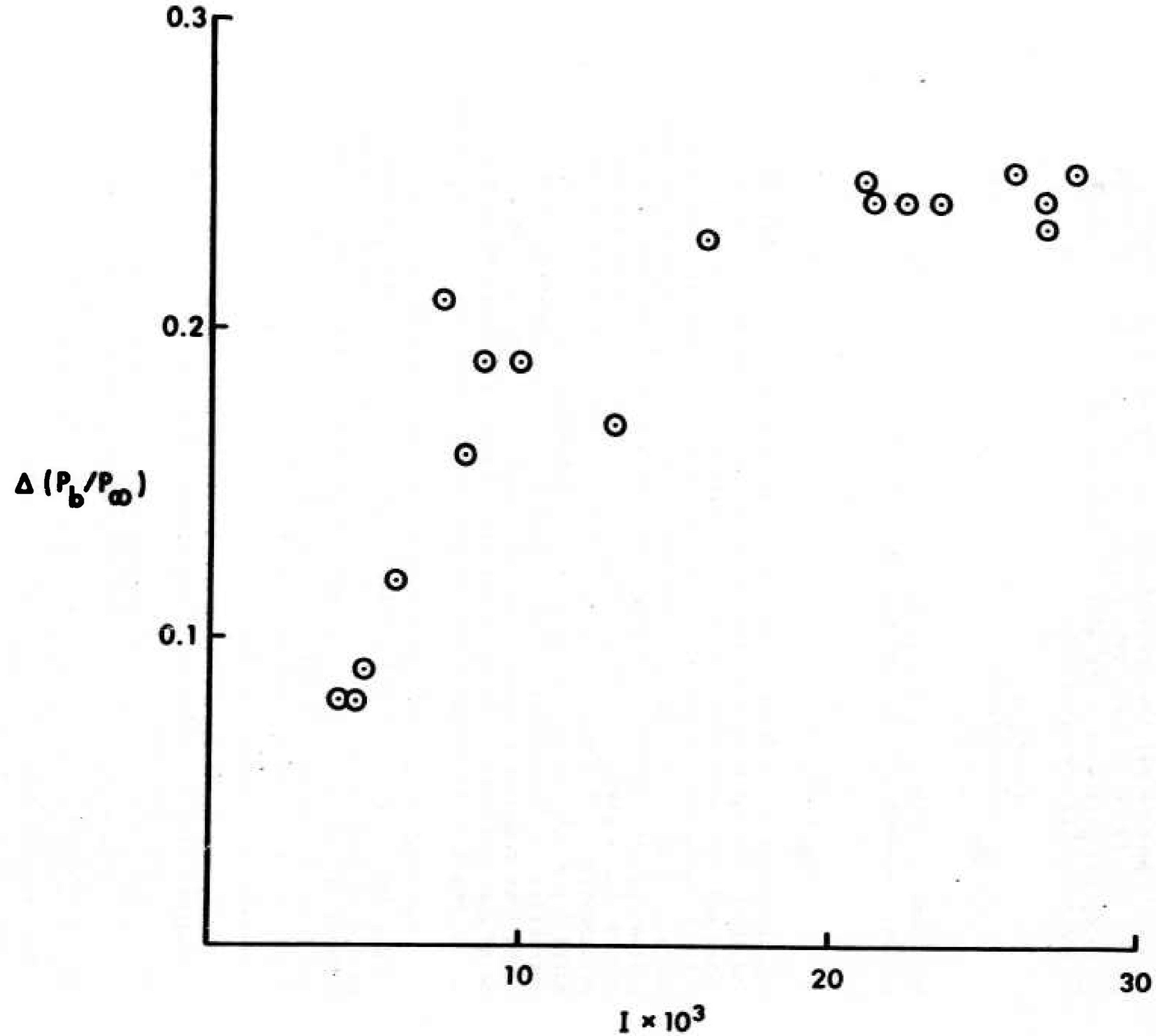

Figure 14. Base Pressure Change _vs_ Injection Parameter for all Runs in Test Series

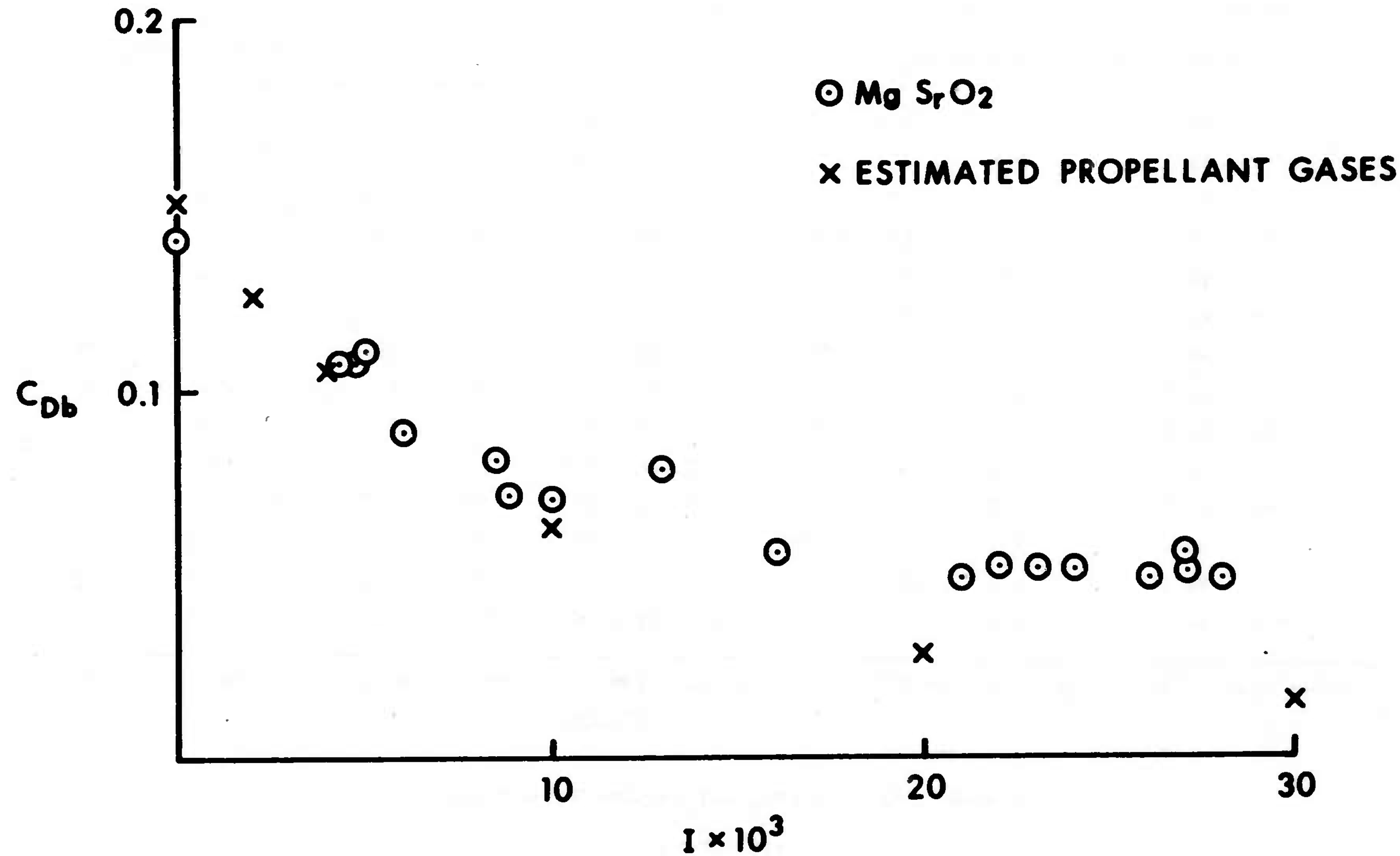

Figure 15. Base Drag Coefficient vs Injection Parameter

TABLE VIII

Injection Parameters for Runs From Reference 5.

Run No.	Fumer	T_∞,K	P_∞,bar	(Pb/P_∞) int	(Pb/P_∞) mod.	tb,sec	m,g	$\dot{m}$,g/sec	I x 10^3	M_∞	spin,krpm
1	R20C	270	1.10	0.60	0.81	2.9	10.8	3.7	7.9	1.98	---
2	R284	271	1.08	.60	.71	9.6	8.1	.84	1.8	1.98	---
3	F-1	267	1.08	.60	.71	6.2	10.6	1.7	3.6	1.98	---
9	Fo4 + 6%CR[a]	274	1.04	.62	.73	8.2	8.2	1.0	2.3	1.98	---
62	R20C	302	0.92	.76	.92	2.6	9.4	3.6	12	1.56	---
63	R20C	302	0.92	.76	.92	0.8	9.4	12	42	1.56	43.5
38	$Mg/Sr(NO_3)_2$[b,c]	281	0.95	.62	.75	4.4	8.4	1.9	4.8	1.98	---
42	" [c]	259	0.53	.52	.74	6.0	8.2	1.4	4.9	2.49	---
27	" [c,d]	274	0.94	.62	.74	6.0	8.0	1.3	3.2	1.98	---
29	" [c,d]	276	0.92	.62	.74	5.5	8.2	1.5	3.8	1.98	---
35	" [c,d]	311	.87	.77	.87	5.4	8.5	1.6	5.9	1.56	---
36	" [c,d]	311	.86	.77	.87	5.5	7.9	1.4	5.2	1.56	---
12	" [d]	277	1.07	.61	.72	7.2	8.9	1.2	2.8	1.98	---
13	" [d]	276	1.07	.61	.72	6.7	8.6	1.3	2.8	1.98	---

[a] calcium resinate

[b] 36.5/ 63.4 percent by weight mixture of Mg & $Sr(NO_3)_2$

[c] preheated to assist ignition

[d] steel washer initially present

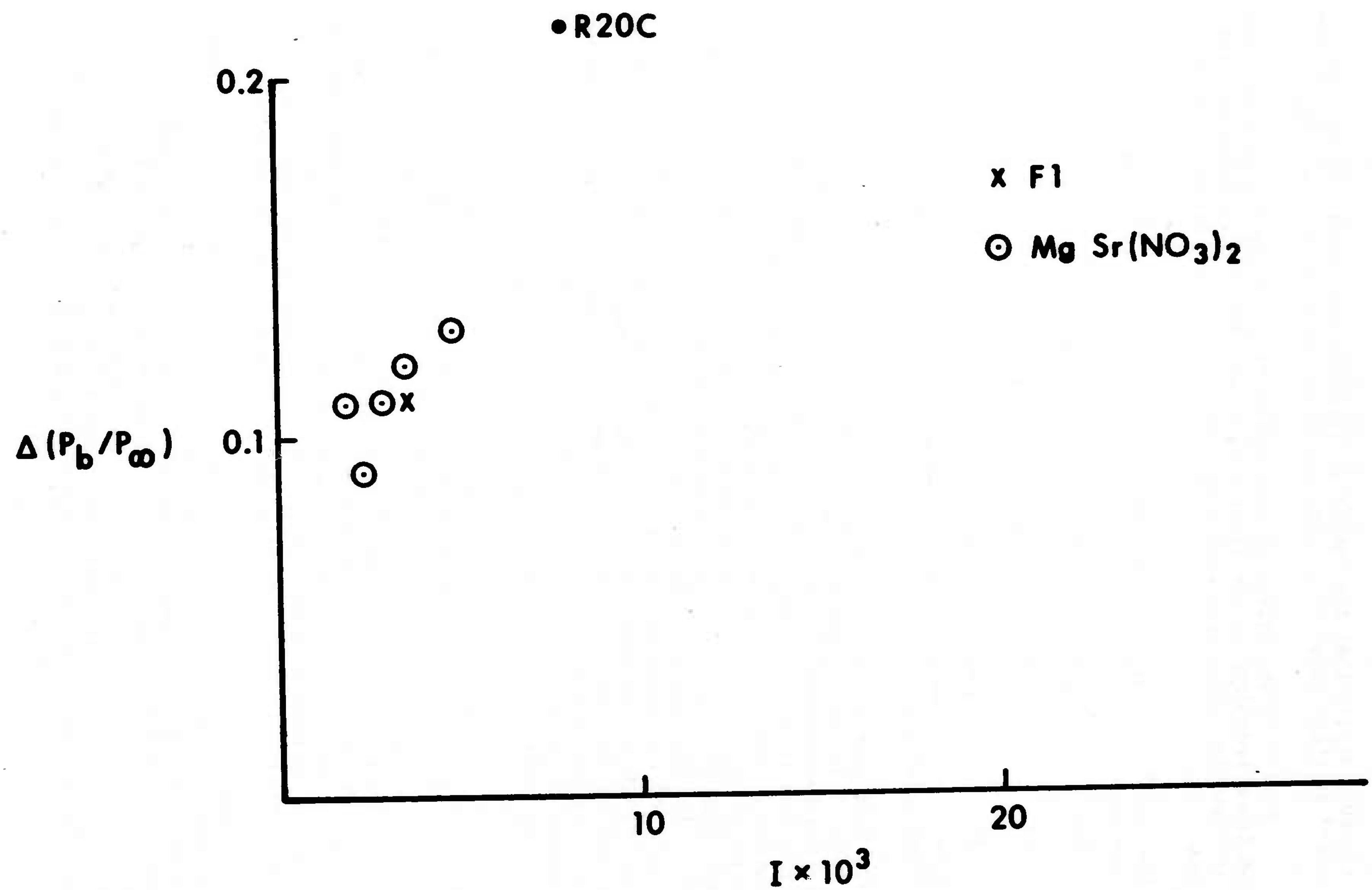

Figure 16. Base Pressure Rise vs Injection Parameter for Mg-$Sr(NO_3)_2$ Mixes

It would appear that the strontium nitrate based fumers follow the same trend as those fumer mixes with strontium peroxide (F-1 and R20C).

A clue to the effect of Mach number on fumer performance may also be found from data in the first wind tunnel report.[5] Tabulated below are data for three runs with a 36.5/63.5 percent by weight $Mg/Sr(NO_3)_2$ mix

Run No. [a]	M_∞	$I \times 10^3$	$\Delta(P_b/P_\infty)$	$\dot{m}$, g/s
36	1.56	5.2	0.10	1.2
12	1.98	2.8	0.11	1.4
42	2.49	4.9	0.22	1.4

[a]From reference 5.

The base pressure rise for a given injection parameter is greatest at the highest Mach number. The same conclusion was reached by previous workers.[9] Although it is difficult to draw firm conclusions from just three runs, the variation in base drag reduction with Mach number is another instance where trends first observed in experiments with gas ejection are also followed by burning pyrotechnics. One should not conclude that it is best to burn the fumer early in projectile flight when the Mach number is the highest. First of all the base drag component of the total drag grows larger at lower Mach numbers[1] and secondly the injection parameter for a given mass burning rate will also get larger at the lower Mach number. From the firing tests conducted parallel to these wind tunnel tests, the largest increase in terminal velocity and reduced flight times after fumer burnout have been seen with the slower burning fumer mixes[4,17] containing strontium nitrate.

One serious discrepancy remains between these results and firing tests reported in Reference 4 as regards the fumer performance of R20C. In these 7.62mm tests, it was concluded that R20C is ineffective as a fumer. Apparently, the R20C completely burns before the round of ammunition is picked up by the radar used to measure the projectile's velocity. Another possibility might be that the rapidly burning R20C masks the radar in some fashion. At any rate it seems odd that R20C provides the largest reduction in base drag observed for any fumer mix in the wind tunnel tests, but exerts no influence at all on base drag in the firing tests.

Another problem that arises when interpreting firing tests without knowledge of the fumer's burn time is to assess relative fumer performance at different Mach numbers when it is possible the fumer has burned out at higher Mach numbers. It is stated in the 7.62mm tests[4] that certain fumer mixes are better than others at higher Mach numbers, but not as effective at lower Mach numbers. In all these cases, the fumer performing better at the higher Mach numbers was the faster burning fumer. It is not clear that F-1, for example, is less effective than R284 at low Mach numbers, since F-1 burns faster than R284. From the limited data available in the wind tunnel tests at different Mach numbers, R20C is superior to the slower-burning $Mg/Sr(NO_3)_2$ mixes at $M_\infty = 2$ and at $M_\infty = 1.56$.

The majority of fumer mixes tested to date have used magnesium as the fuel. This was done because magnesium is relatively easy to ignite, so the fumer mixes tested to date are modifications of existing tracer or illuminating flare mixes. Thus, the fumer mixes already tested could be readily incorporated into munitions and one would expect them to satisfy military storage and handling tests. Future experiments will be directed to other fuel-oxidizer combinations. In particular, attention will be directed to hydrides or compounds producing hydrogen. Townend[23] reported that combustion of hydrogen eliminated base drag at $M_\infty = 2.1$ with injection parameters as low as 0.002. Another advantage of hydrides such as MgH_2, is that their thermal diffusivity[16] is much lower than the thermal diffusivity of the corresponding metal. This means that the metal hydrides should be much easier to ignite. In addition the decomposition of the metal hydride to produce hydrogen occurs endothermically,[24] so the burning rate of a metal-hydride fumer should be slower than the corresponding metal-containing fumer. Metal hydrides such as $NaBH_4$, MgH_2, and ZrH_2 will be tested as fumer fuels.

A final point to be drawn from these results is that in order to take full advantage of the increased performance afforded by fumers, it will require rounds designed to carry larger amounts of fumer mixes, rather than looking for a "best" fumer mix for use in existing tracer rounds.

V. CONCLUSIONS

1. The base drag reduction by burning magnesium-strontium peroxide fumer mixes may be correlated by the same injection parameter previously used to correlate base drag reduction by gas ejection. Such a correlation means that the base drag reduction of a given fumer mix may be estimated solely from an estimate of the mass burning rate under flight conditions.

2. At $M_\infty = 2$ the base drag coefficient is reduced by increasing the injection parameter of the fumer mix up to an injection parameter of 0.02. Similar limits on base drag reduction <u>vs</u> mass flow rate were

---

[23] *L. H. Townend, "Some Effects of Stable Combustion in Wakes Formed in a Supersonic Stream," RAE Technical Note Aero. 2872, March 1963.*

[24] *D. L. Cummings and D. L. Powers, "The Storage of Hydrogen as Metal Hydrides," I & E. C. Process Design and Dev. 13, 182 (1974).*

observed for gas ejection in other wind tunnel tests. One of the major goals of the wind tunnel testing in the fumer program was to see if such limits existed for burning pyrotechnics and propellants.

3. The experimentally measured base drag reductions for magnesium based fumer mixes are the same as the base drag reductions estimated for propellant combustion gases. If such estimates prove to be accurate, this raises the possibility of "invisible" fumer rounds.

4. Center-perforated washers did not influence fumer performance. Such washers were used in firing tests to test the effect on fumer performance when the diameter of the fumer cavity was reduced.

5. Limited data suggest that base drag reduction by a fumer mix with a given injection parameter is more efficient at higher Mach numbers.

ACKNOWLEDGMENT

The authors wish to thank other participants in this program for helpful discussions and the use of recently acquired data. In particular the authors wish to thank Professor S. N. B. Murthy of Purdue University and Mr. Richard Kwatnoski of Frankford Arsenal.

REFERENCES

1. B. J. Reiter, B. B. Grollman, and A. E. Thrailkill, "A Compendium of Ballistic Properties of Projectiles of Possible Interest in Small Arms," BRL Report No. 1532, February 1971. AD# 882117.

2. S. N. B. Murthy and J. R. Osborn, "Base Flow Data With and Without Injection: Bibliography and Semi-Rational Correlations," BRL Contract Report No. 113, August 1973. AD# 914188L.

3. S. N. B. Murthy, J. R. Osborn, J. R. Ward, and A. W. Barrows, eds, Aerodynamics of Base Combustion, MIT Press, Boston, in press.

4. R. Kwatnoski, "Drag-Reducing Fumer For Application in Small Arms Ammunition," Frankford Arsenal Report No. R-3003, March 1974.

5. J. R. Ward, F. P. Baltakis, and S. W. Pronchick, "Wind Tunnel Study of Base Drag Reduction by Combustion of Pyrotechnics," BRL Report No. 1745, October 1974. AD# B000431L.

6. F. P. Baltakis, "Wind Tunnel Study of Projectile Base Drag Reduction Through Combustion of Solid, Fuel-Rich Propellants," NOL Wind Tunnel Report No. 93, October 1974.

7. Engineering Design Handbook, "Military Pyrotechnics Series Part Three-Properties of Materials Used in Pyrotechnic Compositions," AMC Pamphlet AMCP 706-187 October 1963.

8. G. P. Sutton, Rocket Propulsion Elements, 3rd ed., John Wiley and Sons, NY, 1963, p. 40.

9. J. E. Bowman and W. A. Clayden, "Reduction of Base Drag by Gas Ejection," RARDE Report 4/69, December 1969.

10. L. D. Keyser, "Effects of Base Bleed and Supersonic Nozzle Injection on Base Pressure," BRL Memorandum Report No. 2456, March 1975. AD# B003442L.

11. J. J. Caven and T. Stevenson, "Pyrotechnics for Small Arms Ammunition," Frankford Arsenal Report R-1968, July 1970.

12. W. Puchalski, "The Effect of Angular Velocity and Composition on Pyrotechnic Performance," Frankford Arsenal Technical Report 74011, August 1974.

13. D. J. Spring and K. L. Blackwell," Tables for Calculation of Reynolds Number as a Function of Mach Number, Stagnation Pressure, and Stagnation Temperature," US Army Missile Command Report RD-TR-63-3, February 1963.

14. L. Decker and J. R. Ward, "Linear Burning Rates of Pressed Propellants," BRL Memorandum Report in press.

15. J. Reid and R. C. Hastings, "The Effect of a Central Jet on the Base Pressure of a Cylindrical Afterbody in a Supersonic Stream," RAE Report No. Aero. 2621, December 1959.

16. J. R. Ward and R. K. Pahel, "Fuel-Rich Magnesium/Oxidizer Mixes as Drag-Reducing Fumers," BRL Memorandum Report No. 2336, October 1973. AD# 771171.

17. T. A. Elmendorf and R. A. Trifiletti, "Gas Generators for Base Drag Reduction (Fumers)," Aerodynamics of Base Combustion, S. N. B. Murthy et al, eds., HIT Press, Boston, in press.

18. R. Kwatnoski, private communication.

19. I. W. Lyons, The Chemistry and Use of Fire Retardants, Wiley-Interscience, 1970, pp 14-22.

20. D. Hart and H. J. Eppig, "Long Range Research on Pyrotechnics: Burning Characteristics of Binary Mixes," Picatinny Arsenal Technical Report 1669, October 1947.

21. A. A. Shidlovskii, Bases of Pyrotechnics, in Russian, 1964, translated version available as Picatinny Arsenal Technical Memorandum 1615, May 1965.

22. W. J. Puchalski, "An Analysis to Determine the Feasibility of a Non-Luminous Pyrotechnic Fumer," Frankford Arsenal Technical Report-74036, December 1974.

23. L. H. Townend, "Some Effects of Stable Combustion in Wakes Formed in a Supersonic Stream," RAE Technical Note Aero. 2872, March 1963.

24. D. L. Cummings and D. L. Powers, "The Storage of Hydrogen as Metal Hydrides," I & E. C. Process Design and Dev. 13, 182 (1974).

APPENDIX A

Summary of Tests Performed in this Test Series

APPENDIX A.

Summary of Test Conditions

Run No.	M_∞	P_o, bar	T_o, K	Propellant Composition	Remarks
107	1.98	8.07	163		Boundary layer survey
108	1.56	3.8	158		Boundary layer survey
109	1.56	3.9	157		Boundary layer survey
110	2.49	14.1	183		Boundary layer survey
111	2.49	14.2	181		Boundary layer survey
112	1.98	8.41	173		Boundary layer survey
113	1.98	8.62	171		Boundary layer survey
114	1.98	8.27	164		Boundary layer survey
115	1.98	9.03	158		Boundary layer survey
116	1.98	8.27	214		Boundary layer survey
117	1.98	7.83	211	R-20C (See Table 2)	Model extended 6"
118	1.98			R-20C	Model extended 6"
119	1.98	8.27	244	R-20C	Model extended 6"
120	1.98	8.07	261	F-4 (See Table 2)	Model extended 6" No Combust.
121	1.98	8.27	263	R-20C	Model extended 6"
122	1.98	8.34	263	R-20C	Model extended 6"
123	1.98	8.48	240	R-20C	
124	1.98	8.41	243	R-20C	
125	1.98	8.48	247	Mg/SrO_2, 10/90	
126	1.98	8.27	248	Mg/SrO_2, 15/85	
127	1.98	8.27	239	Mg/SrO_2, 20/80	
128	1.98	8.27	237	Mg/SrO_2, 25/75	
129	1.98	8.20	243	Mg/SrO_2, 30/70	No combustion
130	1.98	8.41	242	Mg/SrO_2, 30/70	No combustion
131	1.98	8.34	237	Mg/SrO_2, 30/70	No combustion
132	1.98	8.14	234	Mg/SrO_2, 30/70	
133	1.98	8.27	235	Mg/SrO_2, 35/65	No combustion
134	1.98	8.14	237	Mg/SrO_2, 20/80, Coarse	Delayed ignition
135	1.98	8.00	237	Mg/SrO_2, 20/80, Fire	No combustion

APPENDIX A.

Summary of Test Conditions (Cont'd)

Run No.	M_∞	P_o, bar	T_o, K	Propellant Composition	Remarks
136	1.98	8.14	236	Mg/SrO_2, 20/80	50% area restrict., no comb.
137	1.98	8.00	239	Mg/SrO_2, 20/80	50% area restriction
138	1.98	8.00	242	Mg/SrO_2, 20/80	75% area restriction
139	1.98	8.07	246	Mg/SrO_2, 15/85, 2% Ca Res.	
140	1.98	8.07	244	Mg/SrO_2, 15/85, 4% Ca Res.	
141	1.98	8.00	243	Mg/SrO_2, 15/85, 6% Ca Res.	
142	1.98	8.07	243	Mg/SrO_2, 15/85, 8% Ca Res.	
143	1.98	8.00	242	Mg/SrO_2, 15/85, 10% Ca Res.	
144	1.98	8.20	240	Mg/SrO_2, 15/85, 15% Ca Res.	
145	1.98	8.00	241	Mg/SrO_2, 16.9/83.1	No ignition
146	1.98	8.00	240	Mg/BaO_2, 22.3/77.7	
147	1.98	8.07	237	Mg/SrO_2, 15/85, 5% Oxamide	
148	1.98	8.20	237	Mg/SrO_2, 15/85, 10% Oxamide	
149	1.98	8.14	236	Mg/SrO_2, 15/85, 15% Oxamide	
150	1.98	8.20	235	Mg/SrO_2, 15/85, 10% Gelatin	
151	1.98	8.27	236	Mg/SrO_2, 15/85, 15% Gelatin	
152	1.98	8.34	246	Mg/SrO_2, 20/80	Spin rate 5 → 0 Krpm
153	1.98	8.07	242	R-20C (See Table 2)	Spin rate 35 Krpm
154	1.98	8.14	253	R-20C	Spin rate 11 Krpm
155	1.98	8.07	250	R-20C	Spin rate 30 Krpm
156	1.98	8.20	257	Mg/SrO_2, 10/90	Capsule lost
157	1.98	8.00	257	Mg/SrO_2, 20/80	Capsule not fired
158	1.98	8.41	226	Mg/SrO_2, 20/80	Spin indicator malfunct.
159	1.98	8.27	242	R-20C (See Table 2)	Spin ind. malf., not fired
160	1.98	8.00	236	R-20C	Spin ind. malf., not fired
161	1.98	8.27	246	R-20C	Spin ind. malf.
162	1.98	7.93	259	R-20C	Spin rate 13 Krpm
163	1.98	8.00	261	R-20C	Spin ind. malf., not fired

APPENDIX A.

Summary of Test Conditions (Cont'd)

Run No.	M_∞	P_o, bar	T_o, K	Propellant Composition	Remarks
164	1.98	7.78	269	R-20C	Spin rate 45 Krpm
165	1.98	8.27	271	Mg/SrO_2, 20/80	Spin rate 50 Krpm, no comb.
166	1.98	8.27	272	Mg/SrO_2, 15/85, 5% gelatin	
167	1.98	8.41	275	Mg/SrO_2, 15/85, 5% PVC	DARE malfunction
168	1.98	8.54	271	Mg/SrO_2, 15/85, 10% PVC	
169	1.98	8.41	268	Mg/SrO_2, 15/85, 15% PVC	
170	1.98	8.41	261	Mg/SrO_2, 15/85, 10% polyethylene	
171	1.98	8.34	264	P-1 (See Table 2)	Low luminosity, Spin 14 Krpm
172	1.98	8.27	261	P-1	Low luminosity, Spin 10 Krpm
173	1.98	8.27	250	P-3 (See Table 2)	Decayed ignition, Spin 15 Krpm
174	1.98	8.34	258	P-3	Decaying spin, 18 $\rightarrow$ 5 Krpm
175	1.98	8.27	261	P-7 (See Table 2)	Spin rate 5 Krpm
176	1.98	8.27	264	P-13 (See Table 2)	Spin rate 9 Krpm, No ignition
177	1.98	8.27	256	P-19 (See Table 2)	Spin rate 9 Krpm, No ignition
178	1.98	8.27	250	P-11 (See Table 2)	Spin rate 10 Krpm, No ignition
179	1.98	8.27	253	P-7	Spin rate 12 Krpm
180	1.98	8.27	253	P-9 (See Table 2)	Low lumin., var. spin, 20 $\rightleftarrows$ 20 Krpm
181	1.98	8.00	253	P-17 (See Table 2)	No Lumin., var. spin. 15 $\rightarrow$ 10 Krpm
182	1.98	8.27	253	P-5 (See Table 2)	Incomplete ignition, spin 10 Krpm
183	1.98	8.41	250	P-17	No lumin., var, spin, 15 $\rightarrow$ 6 Krpm
184	1.98	8.07	252	P-15 (See Table 2)	Spin rate 10 Krpm, no ignition
185	1.98	8.00	244	R-20C/R-284	Spin ind. malfunct.
186	1.98	8.00	235	R-20C/R-284	Spin rate 54 Krpm
187	1.98	7.93	233	R-20C/R-284	Spin rate 43 $\rightarrow$ 38 Krpm
188	1.98	8.27	239	Mg/SrO_2, 10/90	Spin rate 45 Krpm, no ignition
189	1.98	8.07	231	R-20C (See Table 2)	Spin rate 45 Krpm
190	1.98	7.93	225	R-20C	Spin rate 52 Krpm
191	1.98	8.00	228	Mg/SrO_2, 10/90	Spin rate 40 Krpm, No ignition

APPENDIX A.

Summary of Test Conditions (Cont'd)

Run No.	M_∞	P_o, bar	T_o, K	Propellant Composition	Remarks
192	1.98	8.00	227	Mg/BaO_2, 15/85, 6% Ca Res.	
193	1.98	8.07	228	Mg/BaO_2, 15/85, 10% Ca Res.	
194	1.98	8.00	225	Mg/BaO_2, 15/85, 15% Ca Res.	
195				R-20C (See Table 2)	Force bal. calibration
196	1.98	8.07	269	R-20C	Force test, balance malf.
197	1.98	8.14	272	R-20C	Force test
198	1.98	8.27	278	R-20C	Force test, balance malf.
199	1.98	7.93	281	R-20C	Force test
200	1.98	7.93	282	R-20C	Force test, balance malf.
201	1.98	8.27	281	R-20C	Force and temp., balance malf.
202	1.98	8.41	275	R-20C	Force and Temp., balance malf.

APPENDIX B

(P_b/P_∞) vs Time Curves For All Runs in This Test Series During Which Burning Took Place

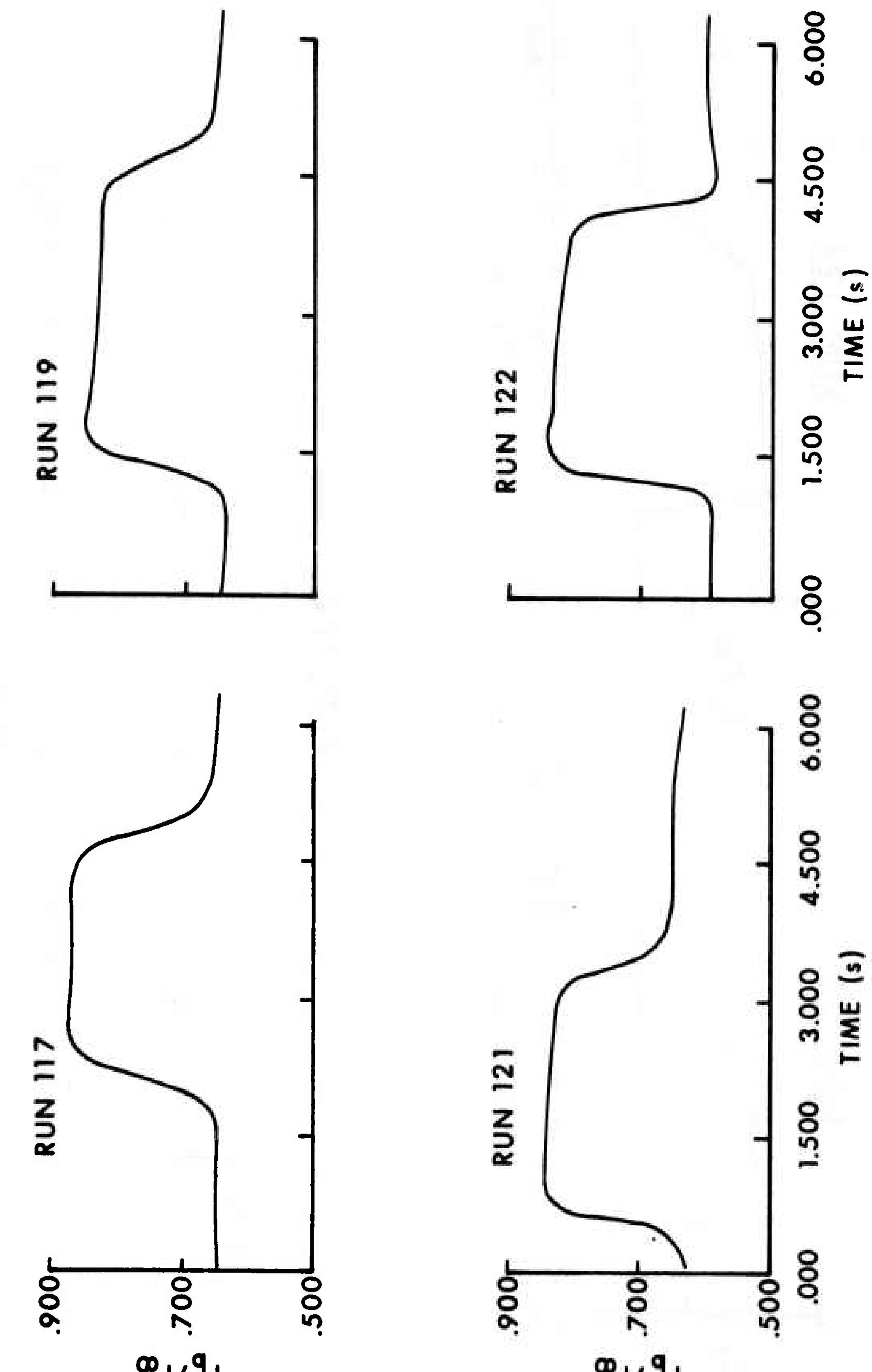
RUN 117
RUN 119
RUN 121
RUN 122
p_b/p_∞
p_b/p_∞
.900
.700
.500
.900
.700
.500
.000
1.500
3.000
4.500
6.000
TIME (s)
.000
1.500
3.000
4.500
6.000
TIME (s)

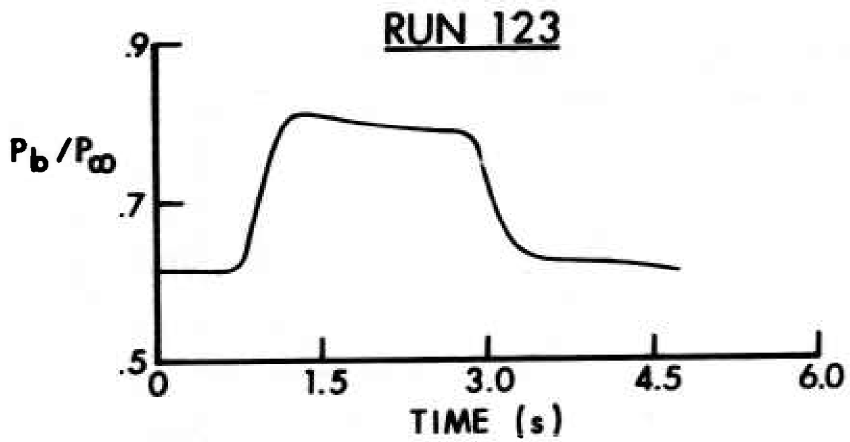
RUN 123
.9
.7
.5
P_b/P_∞
0
1.5
3.0
4.5
6.0
TIME (s)

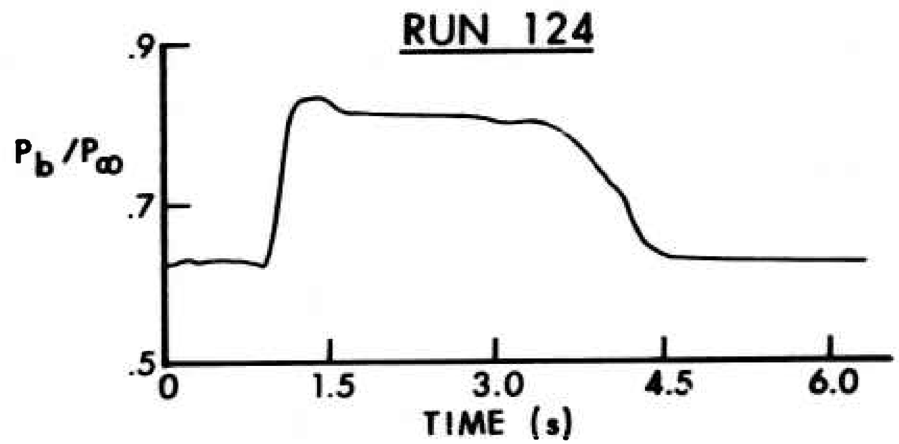
RUN 124
.9
.7
.5
P_b/P_∞
0
1.5
3.0
4.5
6.0
TIME (s)

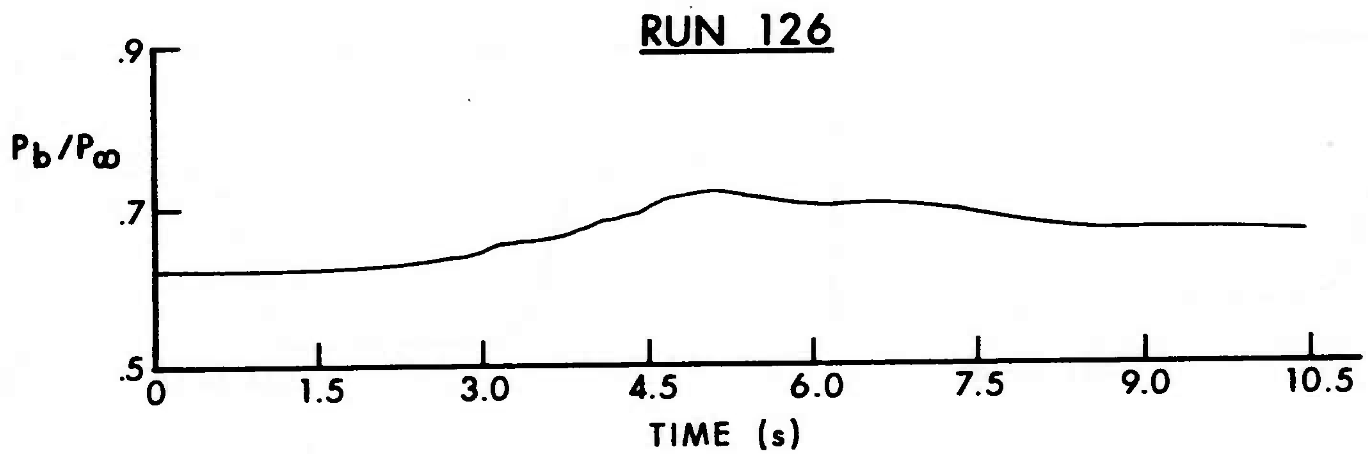
RUN 126
.9
.7
.5
P_b/P_∞
0
1.5
3.0
4.5
6.0
7.5
9.0
10.5
TIME (s)

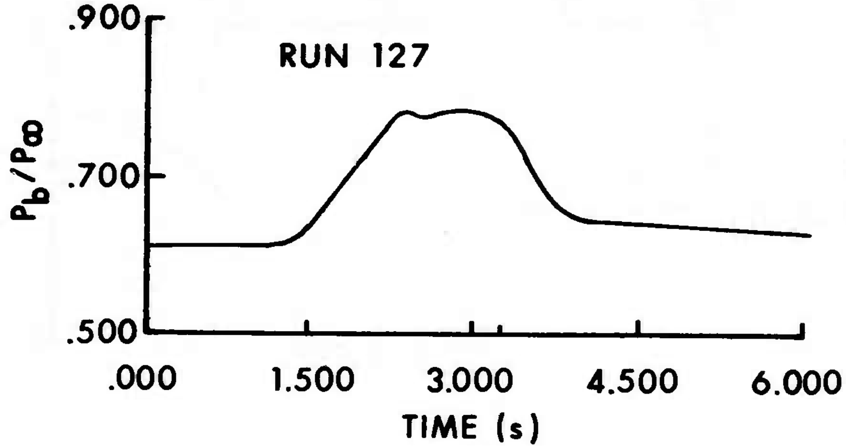
RUN 127
P_b/P_∞
.900
.700
.500
.000
1.500
3.000
4.500
6.000
TIME (s)

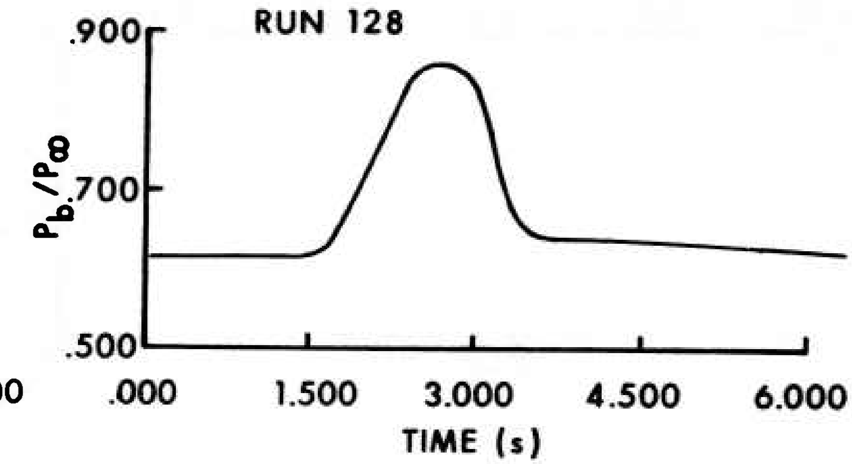
RUN 128
P_b/P_∞
.900
.700
.500
.000
1.500
3.000
4.500
6.000
TIME (s)

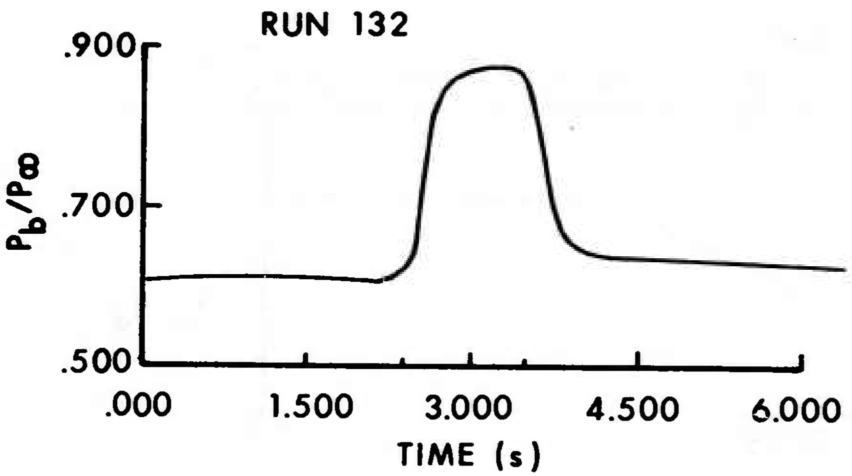
RUN 132
P_b/P_∞
.900
.700
.500
.000
1.500
3.000
4.500
6.000
TIME (s)

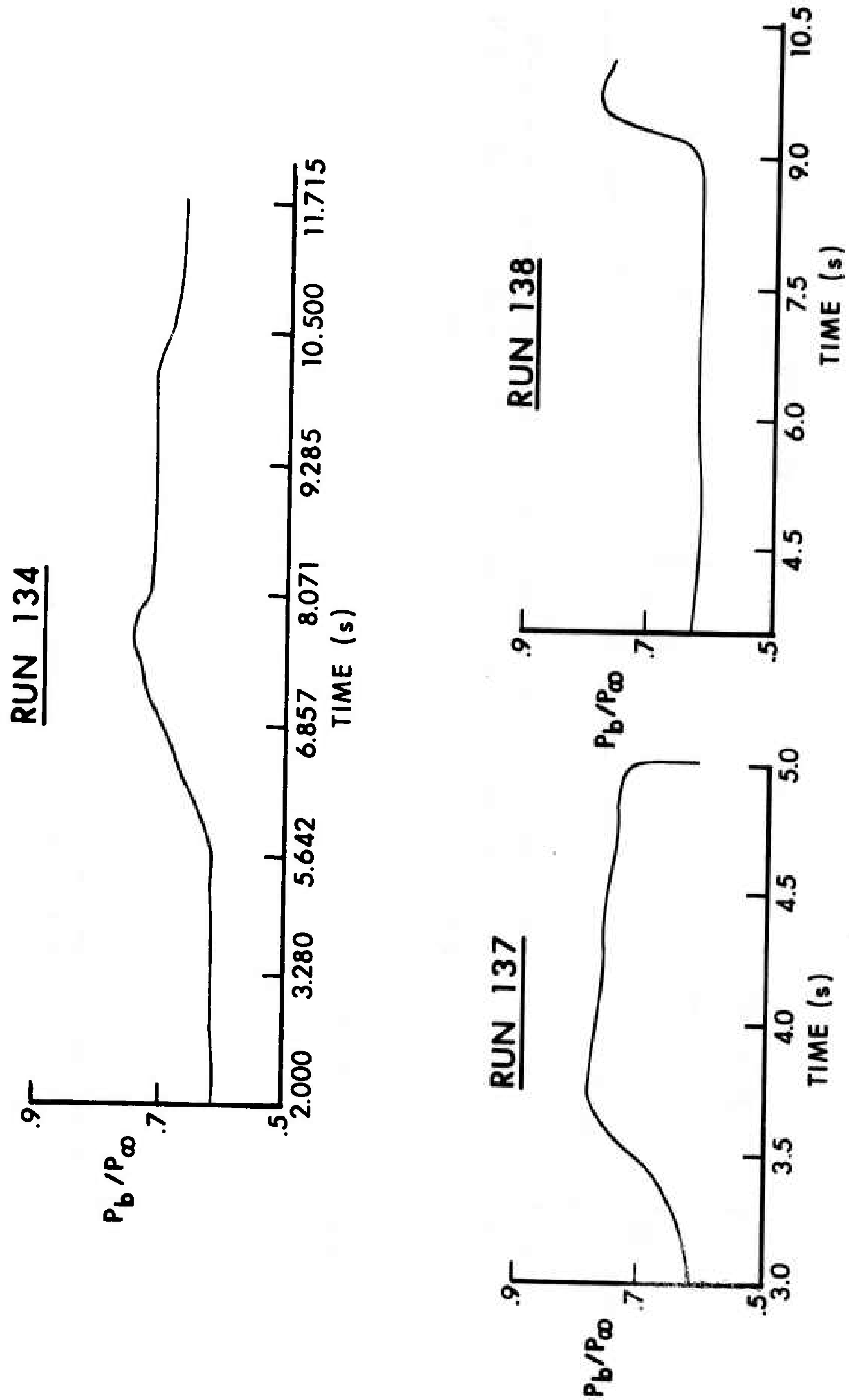
RUN 134
P_b/P_∞
.9
.7
.5
2.000
3.280
5.642
6.857
8.071
9.285
10.500
11.715
TIME (s)
RUN 137
P_b/P_∞
.9
.7
.5
3.0
3.5
4.0
4.5
5.0
TIME (s)
RUN 138
P_b/P_∞
.9
.7
.5
4.5
6.0
7.5
9.0
10.5
TIME (s)

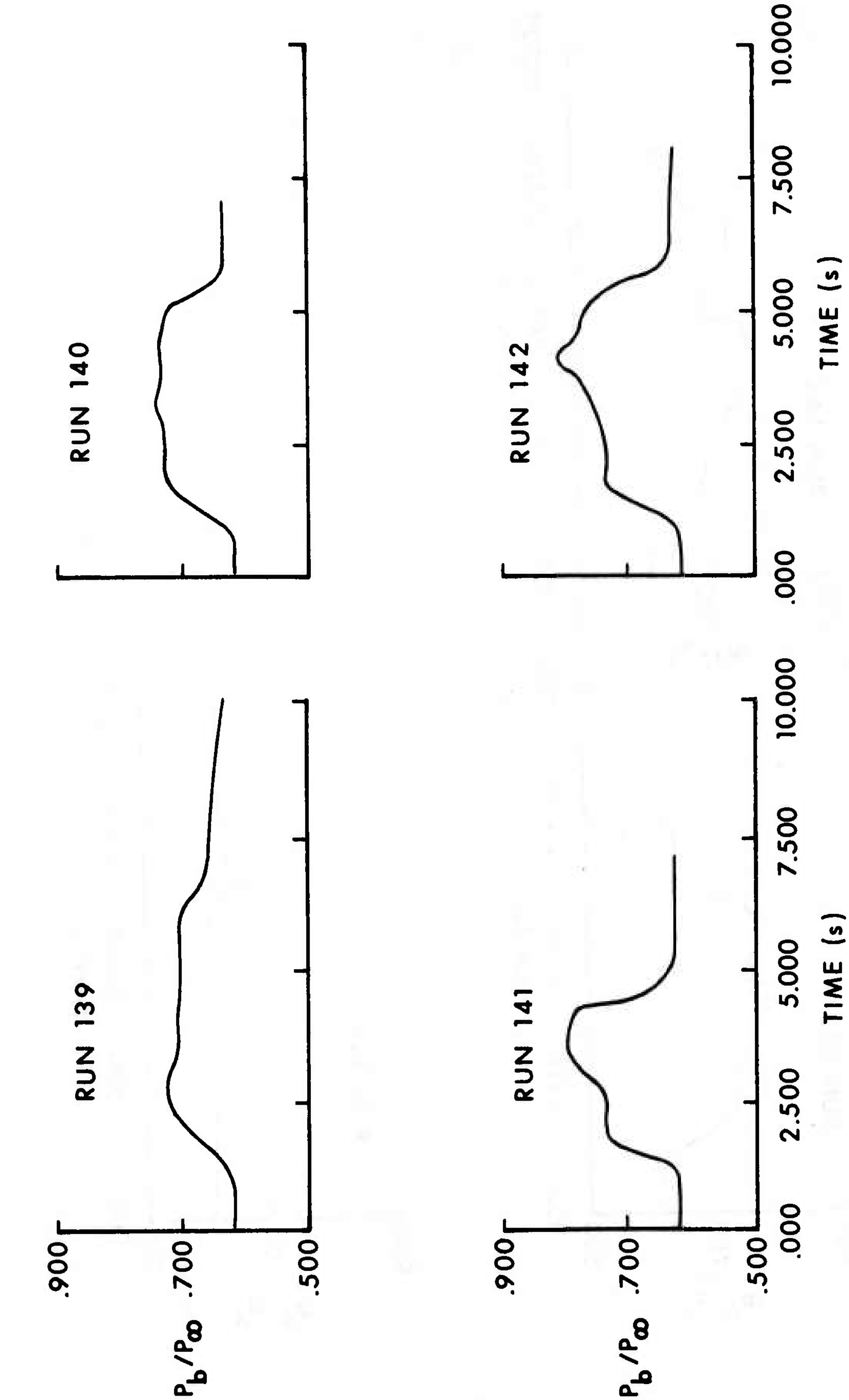
RUN 139
RUN 140
RUN 141
RUN 142
P_b/P_∞
P_b/P_∞
.900
.700
.500
.900
.700
.500
.000
2.500
5.000
7.500
10.000
.000
2.500
5.000
7.500
10.000
TIME (s)
TIME (s)

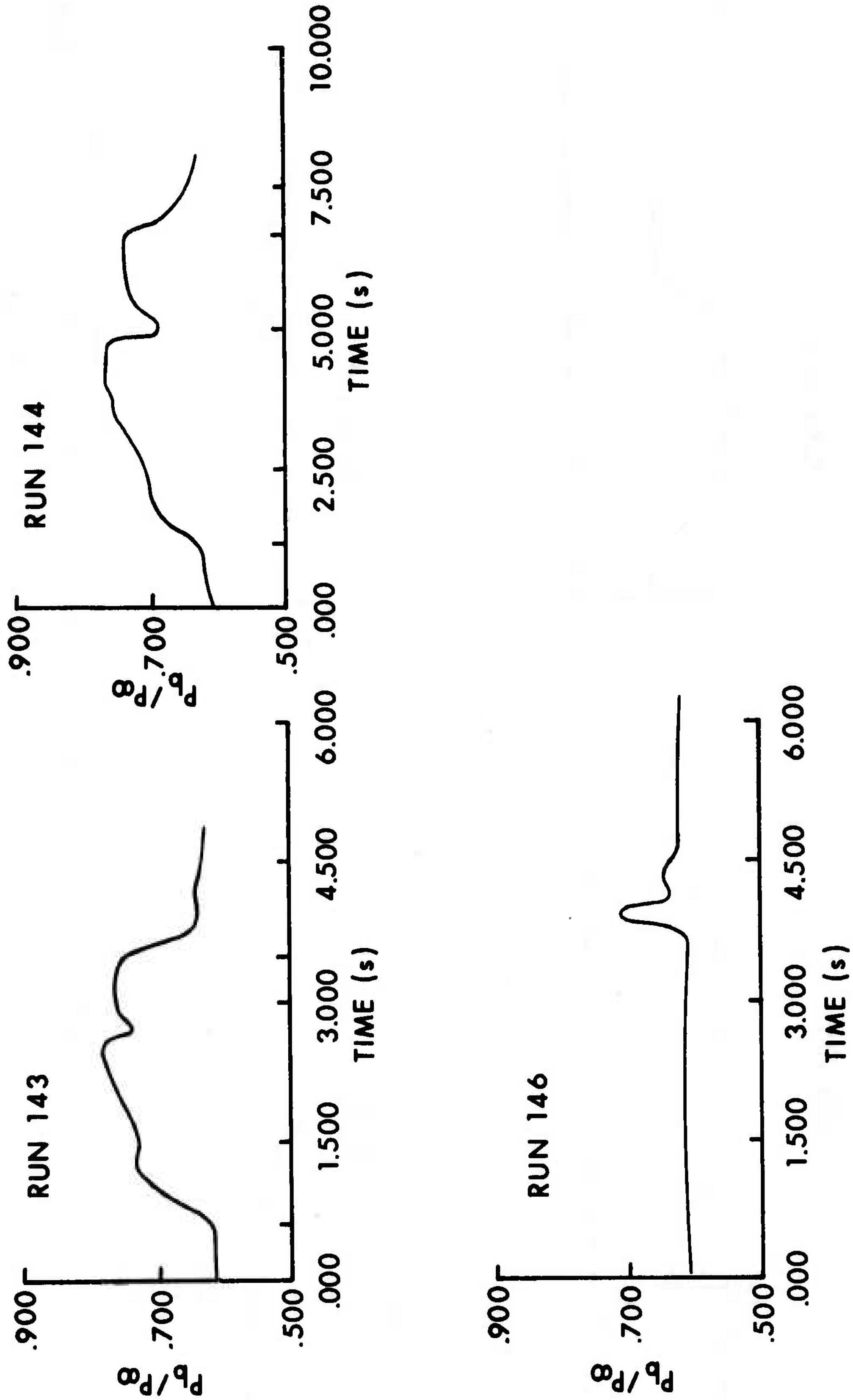
RUN 144
p_b/p_∞
.900
.700
.500
.000
2.500
5.000
7.500
10.000
TIME (s)
RUN 143
p_b/p_∞
.900
.700
.500
.000
1.500
3.000
4.500
6.000
TIME (s)
RUN 146
p_b/p_∞
.900
.700
.500
.000
1.500
3.000
4.500
6.000
TIME (s)

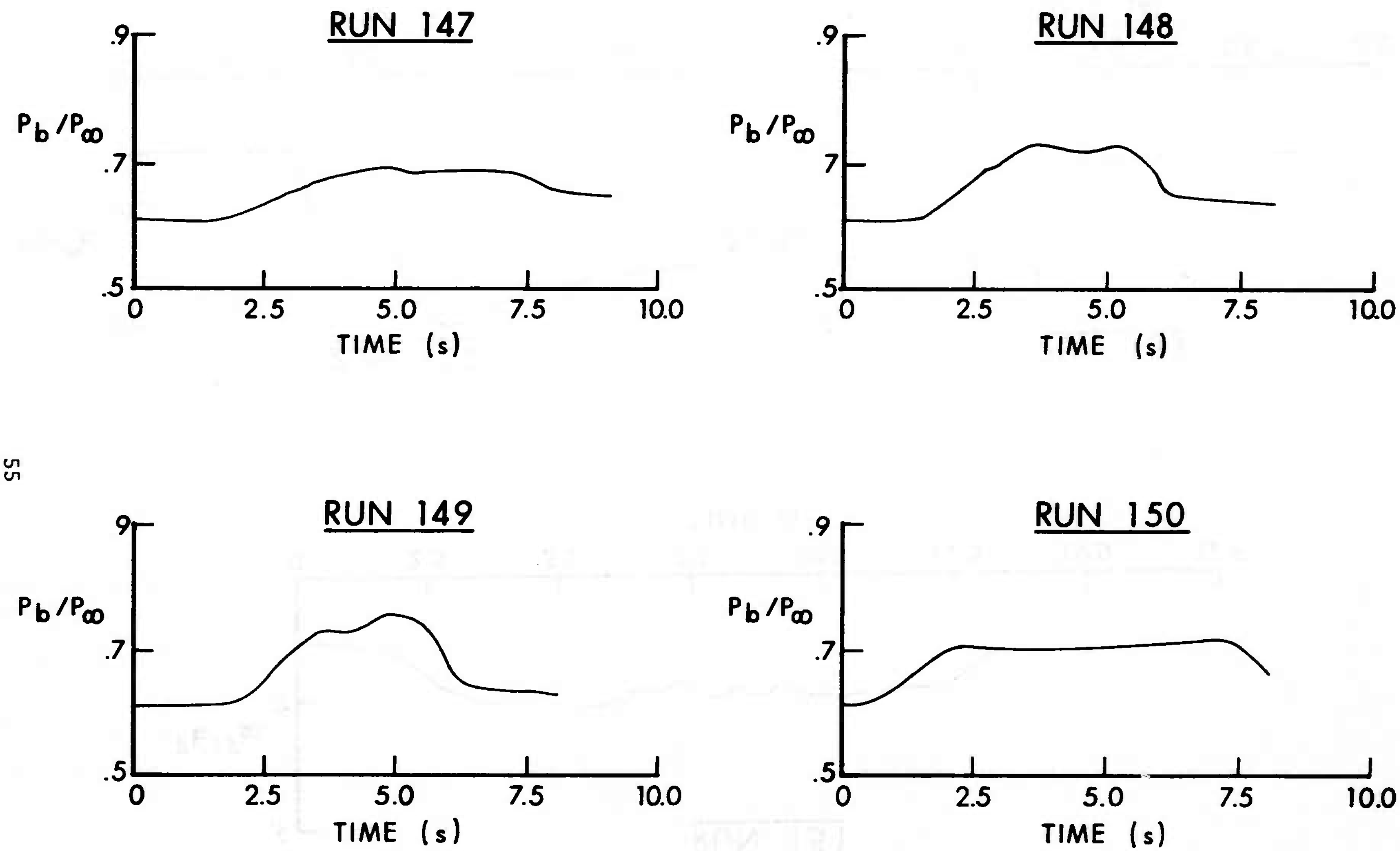
RUN 147
RUN 148
RUN 149
RUN 150
P_b/P_∞
.9
.7
.5
0
2.5
5.0
7.5
10.0
TIME (s)

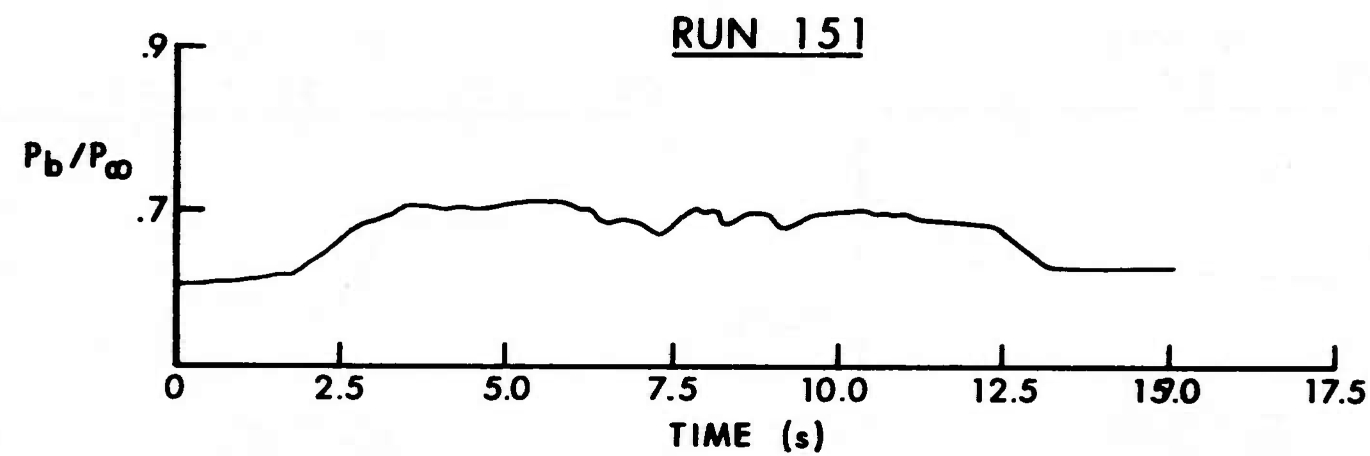
RUN 151
.9
.7
P_b/P_∞
0
2.5
5.0
7.5
10.0
12.5
15.0
17.5
TIME (s)

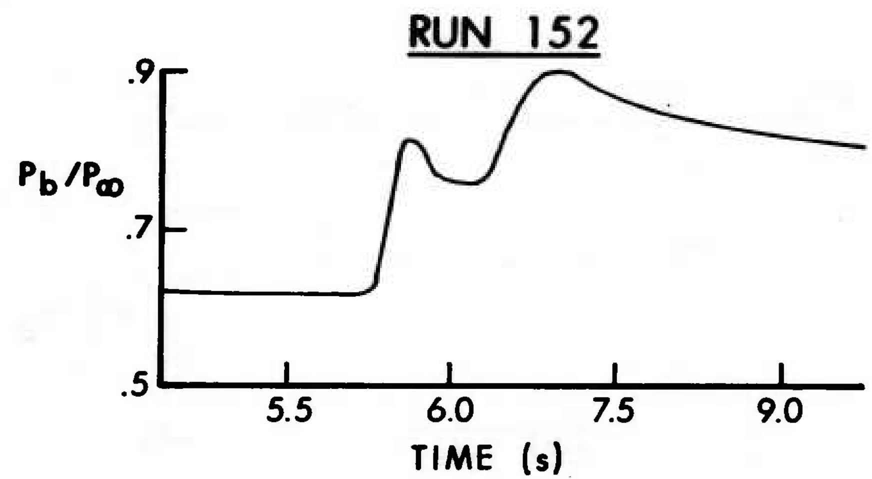
RUN 152
.9
.7
.5
P_b/P_∞
5.5
6.0
7.5
9.0
TIME (s)

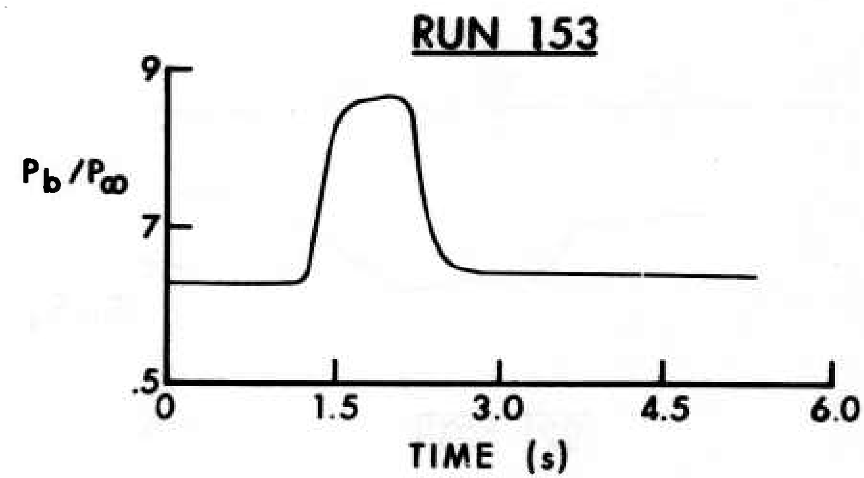
RUN 153
9
7
.5
P_b/P_∞
0
1.5
3.0
4.5
6.0
TIME (s)

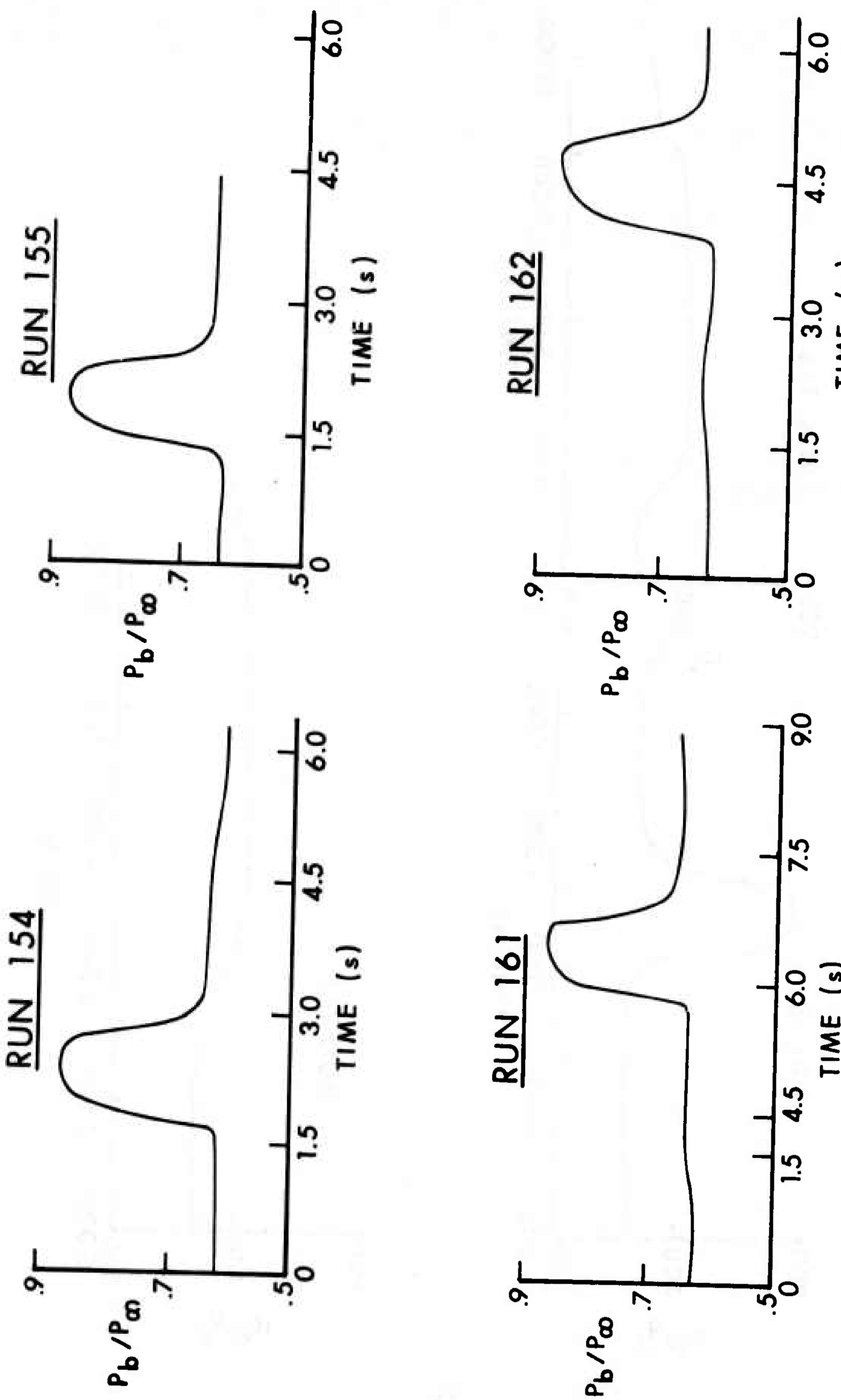
RUN 155
RUN 154
RUN 162
RUN 161
P_b/P_∞
.9
.7
.5
0
1.5
3.0
4.5
6.0
7.5
9.0
TIME (s)

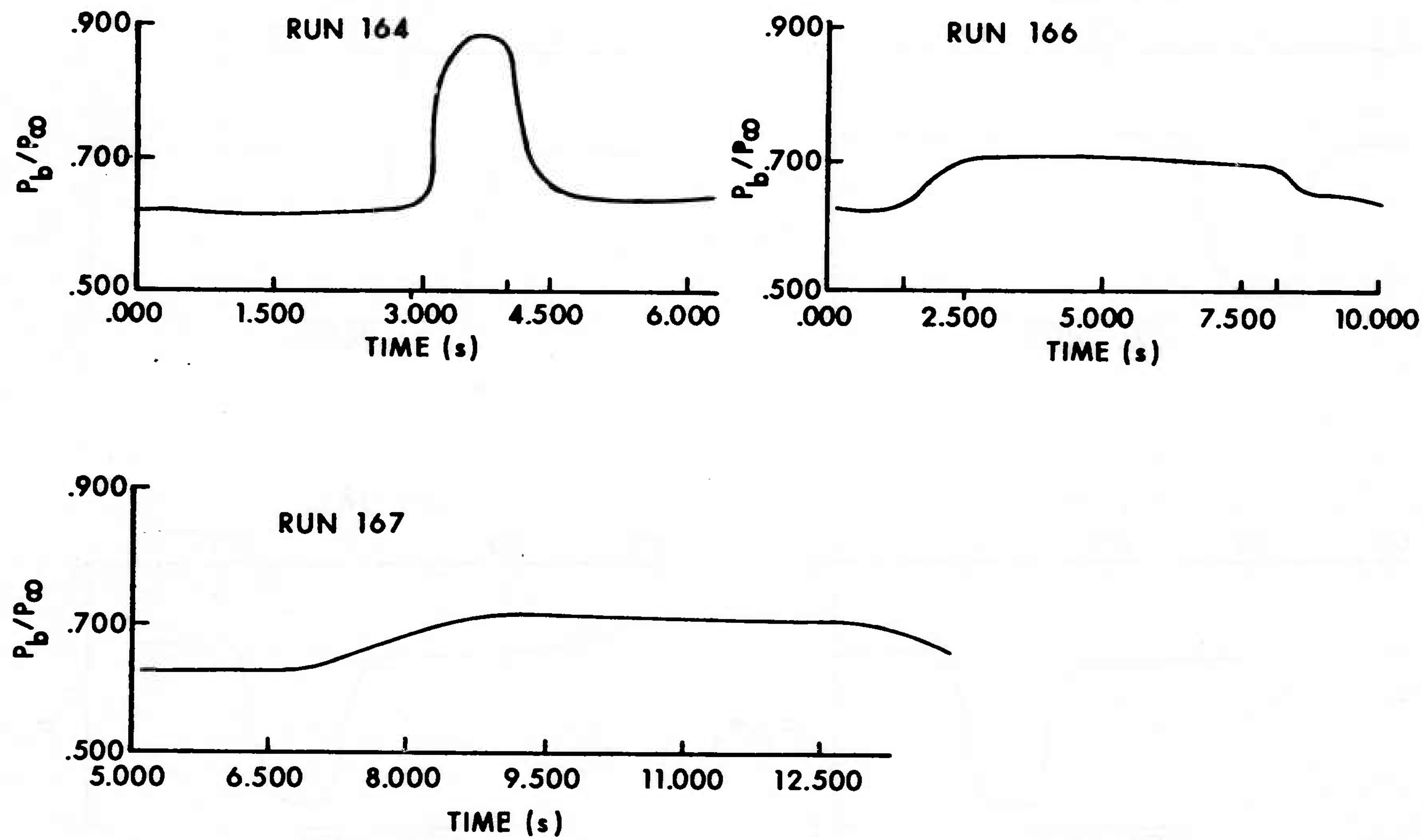
RUN 164
.900
.700
.500
P_b/P_∞
.000
1.500
3.000
4.500
6.000
TIME (s)
RUN 166
.900
.700
.500
P_b/P_∞
.000
2.500
5.000
7.500
10.000
TIME (s)
RUN 167
.900
.700
.500
P_b/P_∞
5.000
6.500
8.000
9.500
11.000
12.500
TIME (s)

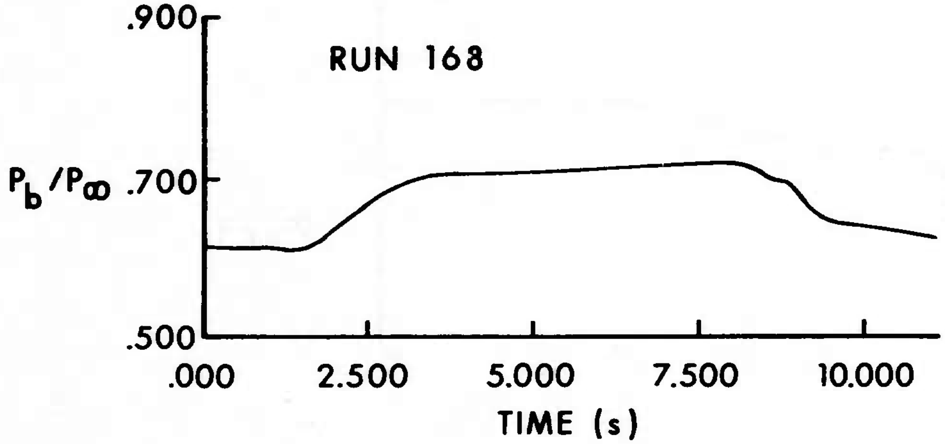
RUN 168
P_b/P_∞
.900
.700
.500
.000
2.500
5.000
7.500
10.000
TIME (s)

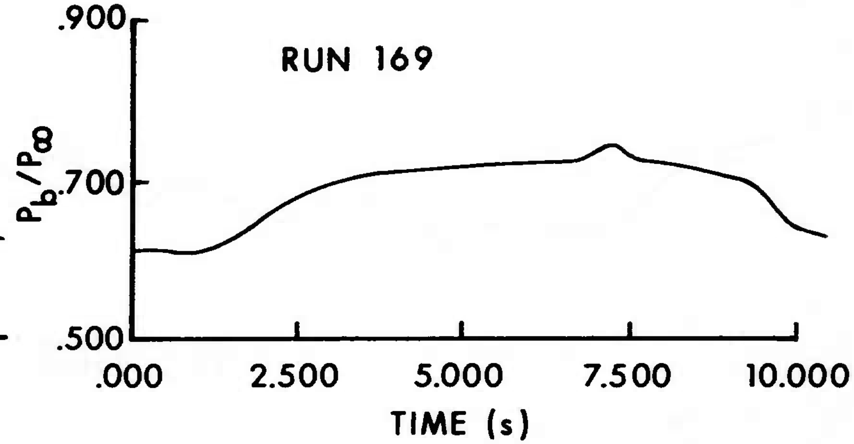
RUN 169
P_b/P_∞
.900
.700
.500
.000
2.500
5.000
7.500
10.000
TIME (s)

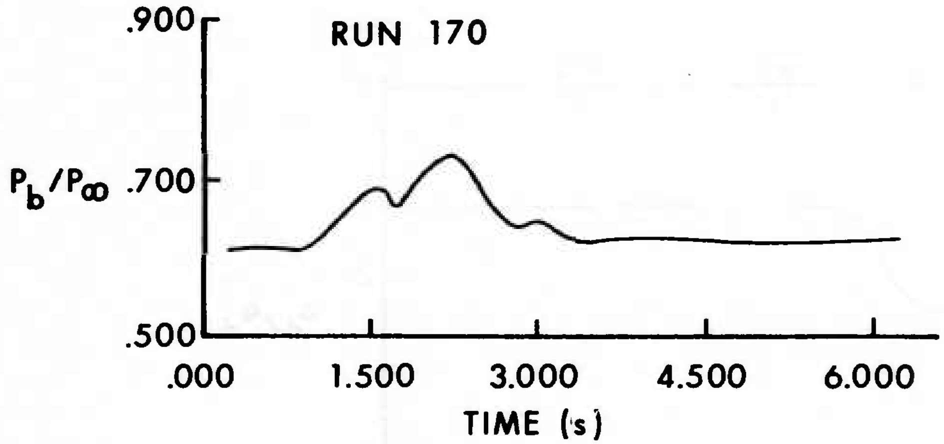
RUN 170
P_b/P_∞
.900
.700
.500
.000
1.500
3.000
4.500
6.000
TIME (s)

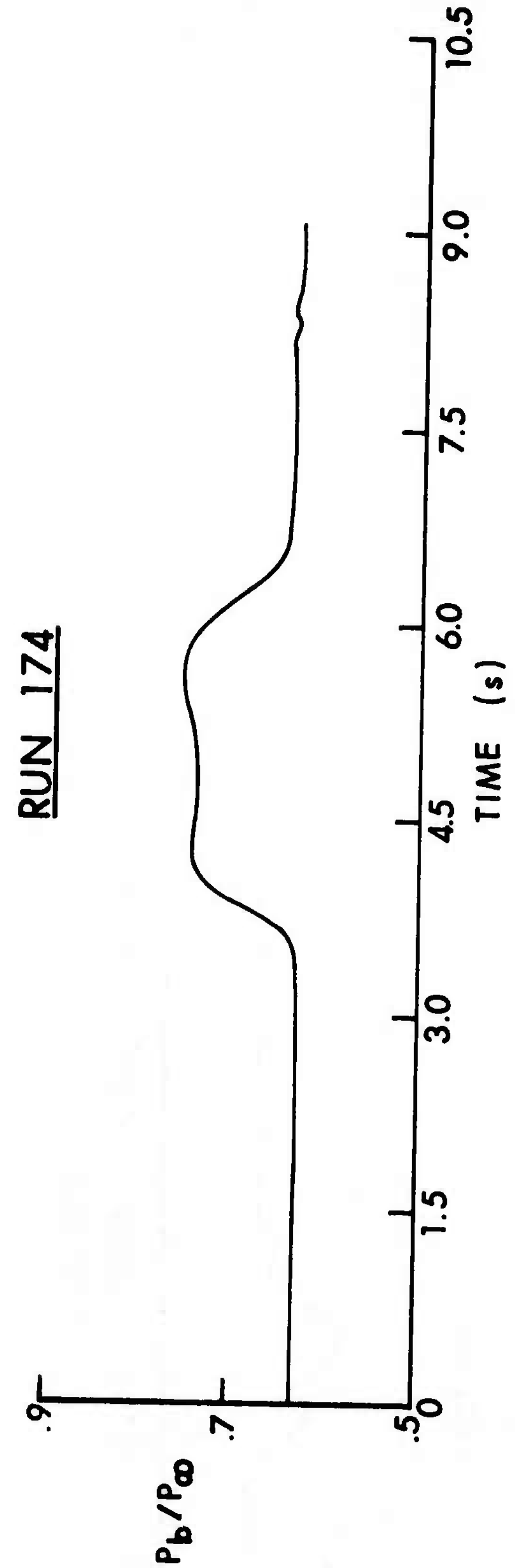

RUN 174
P_b/P_∞
.9
.7
.5
0
1.5
3.0
4.5
6.0
7.5
9.0
10.5
TIME (s)

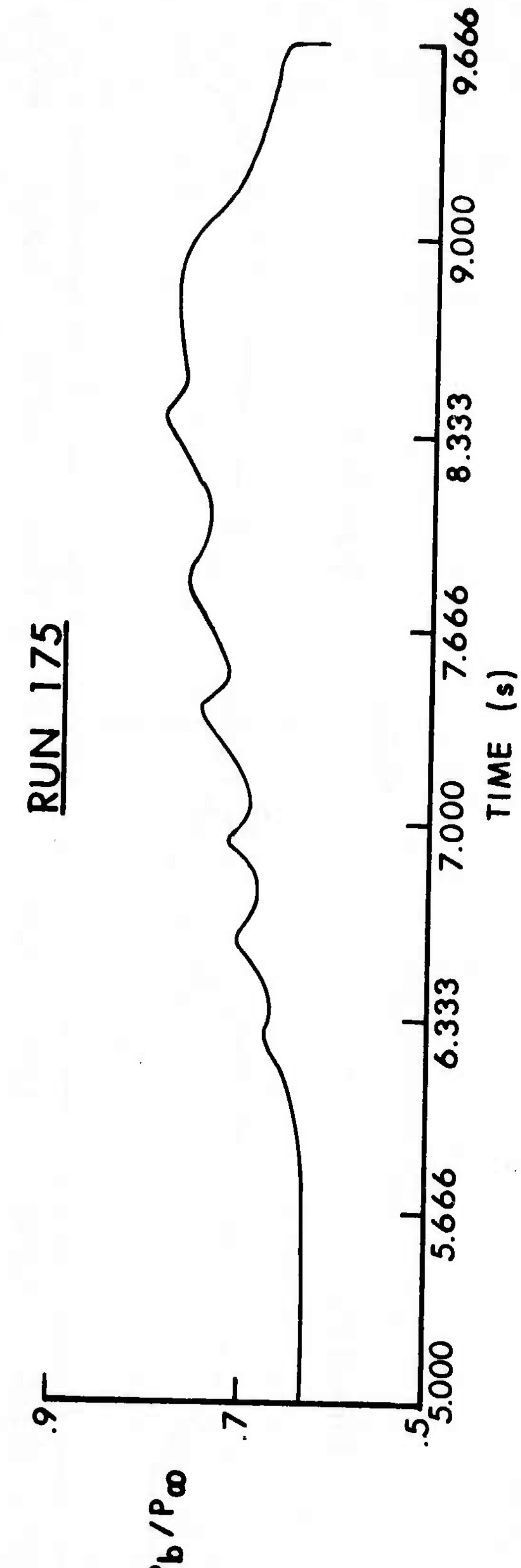

RUN 175
P_b/P_∞
.9
.7
.5
5.000
5.666
6.333
7.000
7.666
8.333
9.000
9.666
TIME (s)

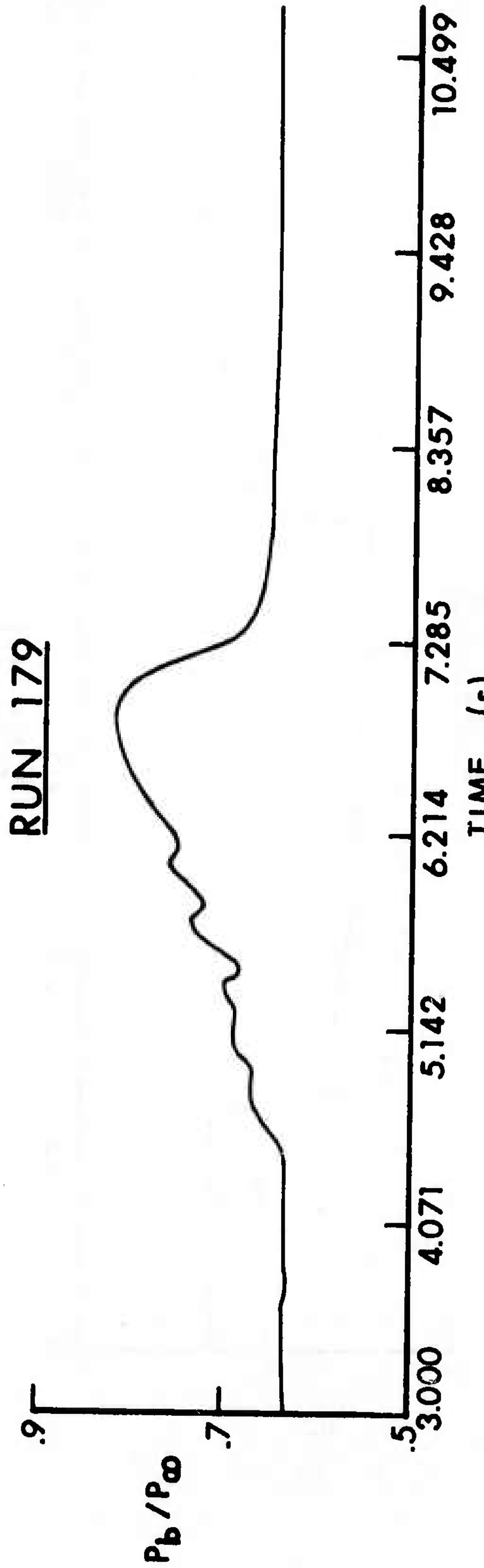
RUN 179
P_b/P_∞
.9
.7
.5
3.000
4.071
5.142
6.214
7.285
8.357
9.428
10.499
TIME (s)

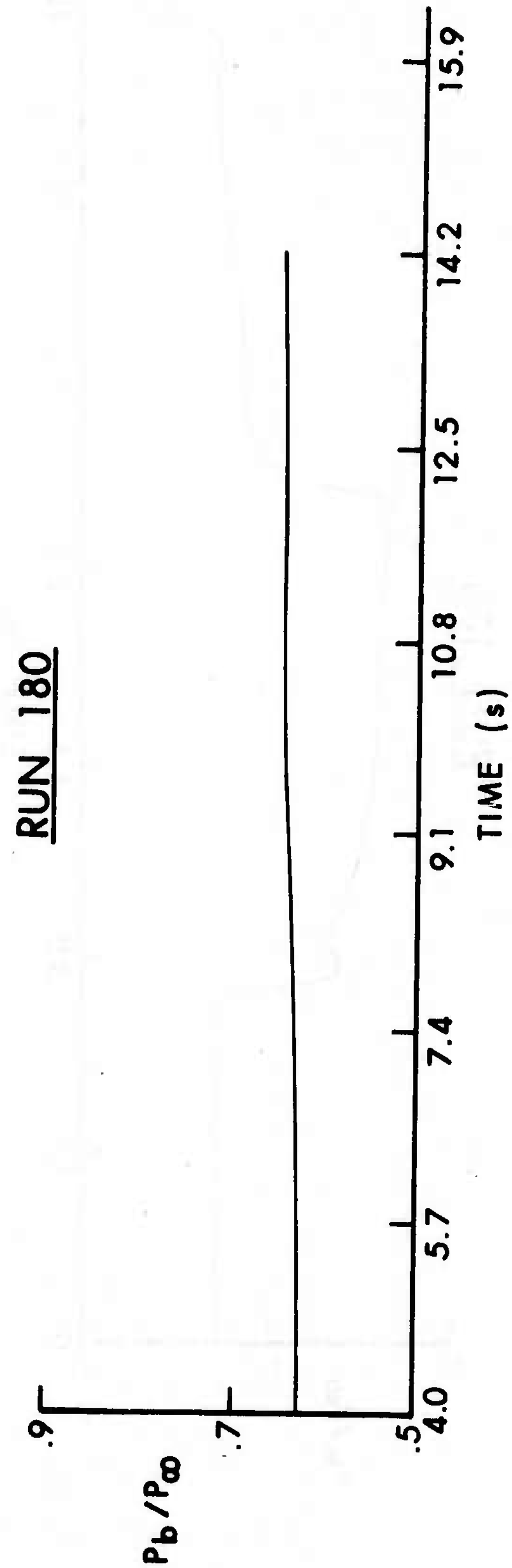
RUN 180
P_b/P_∞
.9
.7
.5
4.0
5.7
7.4
9.1
10.8
12.5
14.2
15.9
TIME (s)

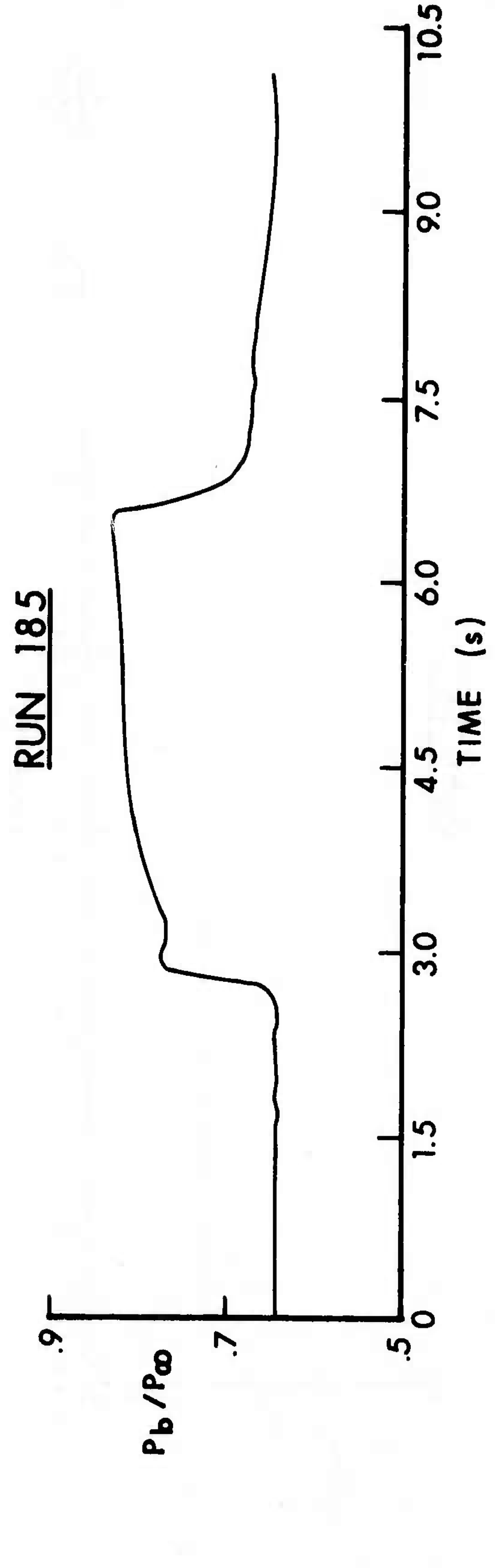
RUN 185
P_b/P_∞
.9
.7
.5
0
1.5
3.0
4.5
6.0
7.5
9.0
10.5
TIME (s)

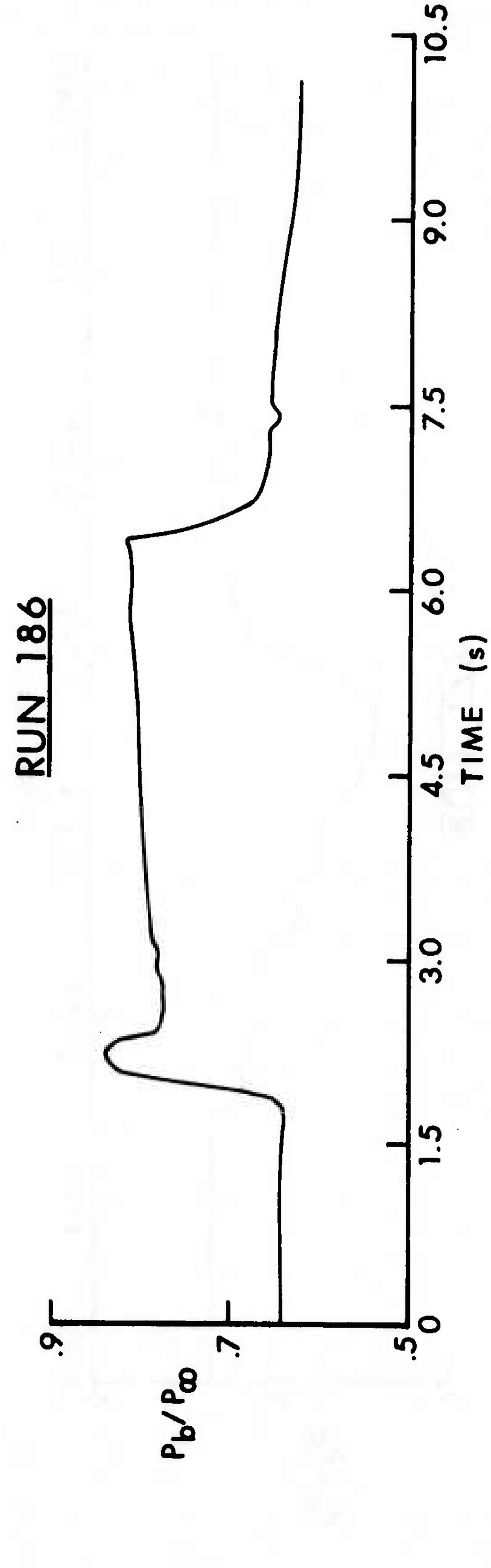
RUN 186
P_b/P_∞
.9
.7
.5
0
1.5
3.0
4.5
6.0
7.5
9.0
10.5
TIME (s)

RUN 181

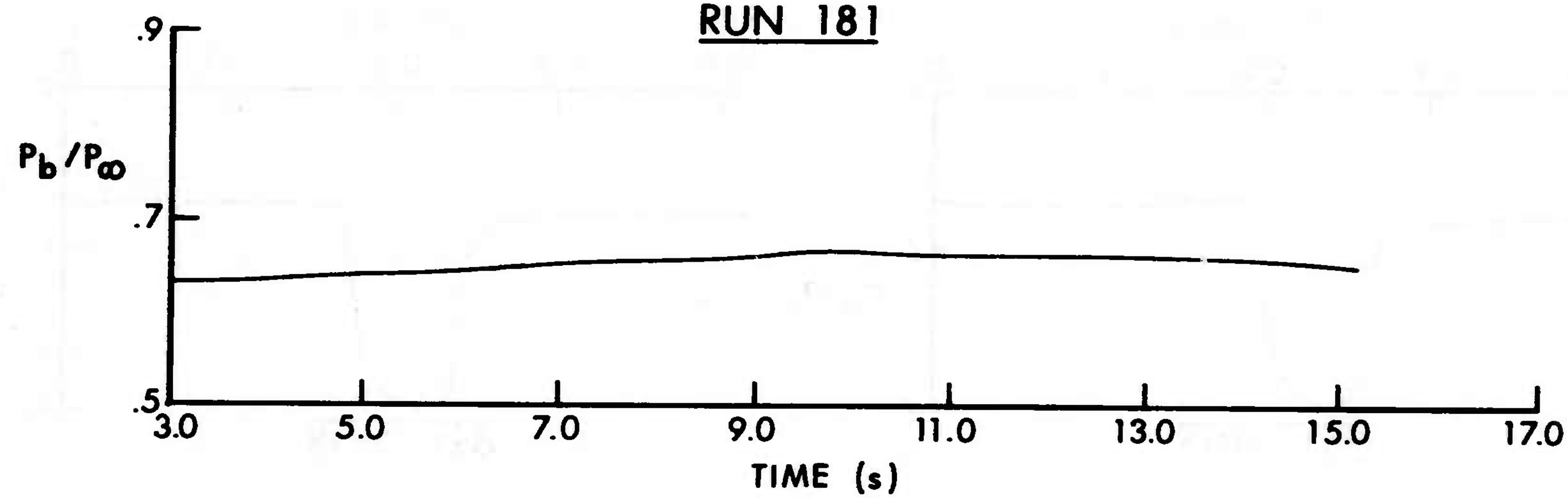

RUN 183

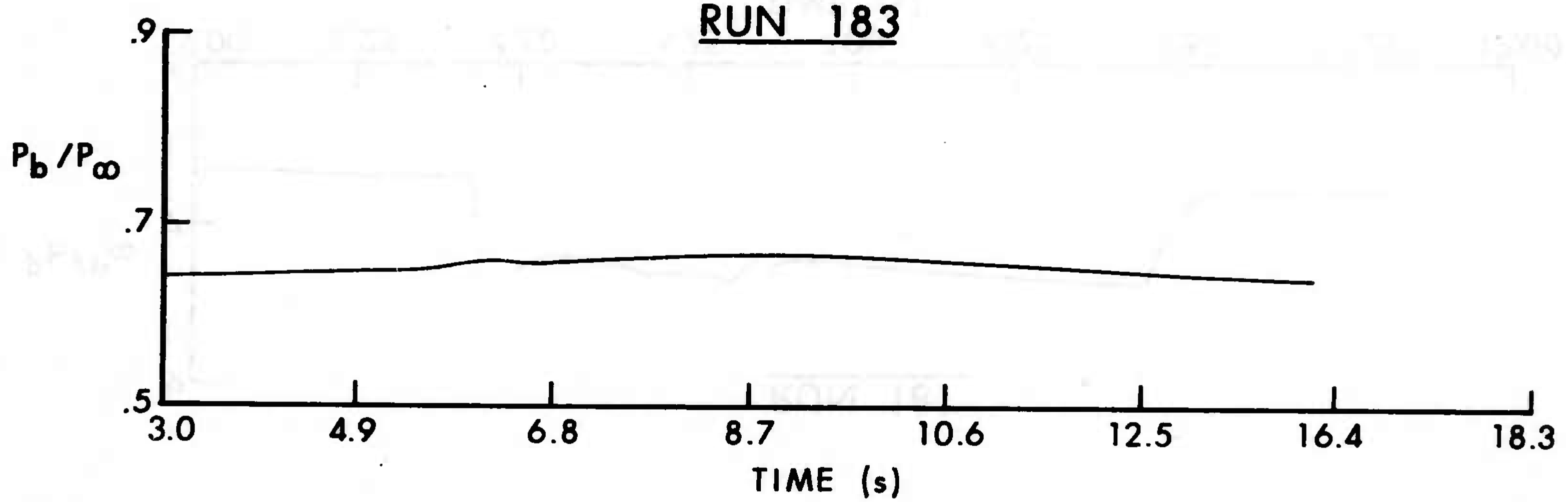

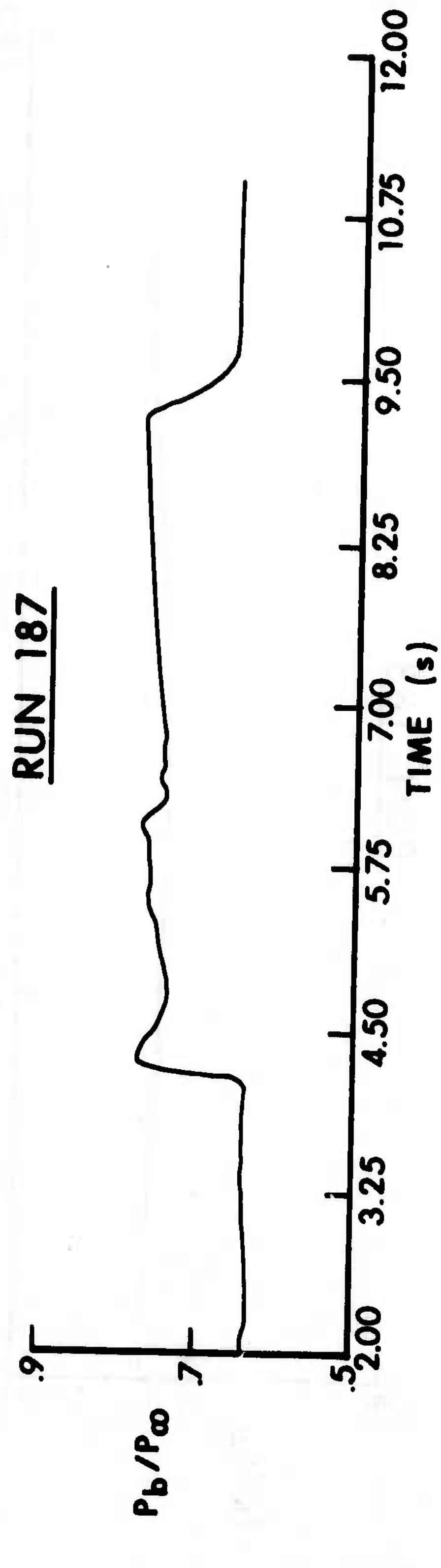
RUN 187
P_b/P_∞
.9
.7
.5
2.00
3.25
4.50
5.75
7.00
8.25
9.50
10.75
12.00
TIME (s)

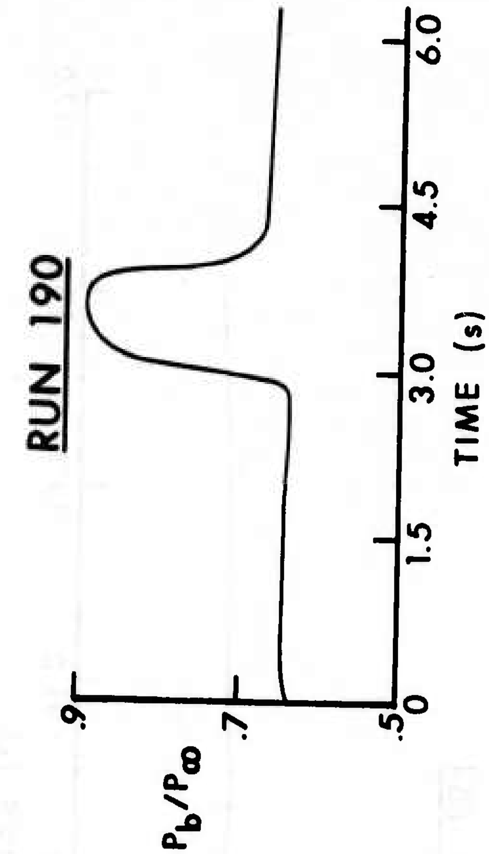
RUN 190
P_b/P_∞
.9
.7
.5
0
1.5
3.0
4.5
6.0
TIME (s)

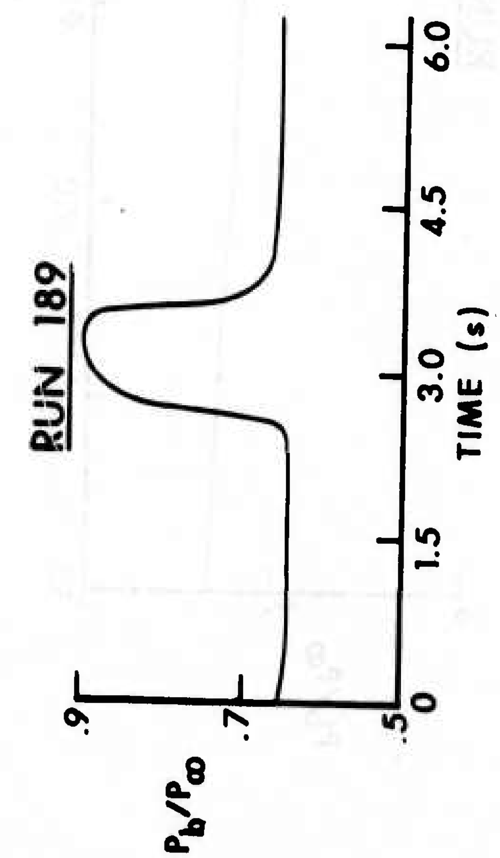
RUN 189
P_b/P_∞
.9
.7
.5
0
1.5
3.0
4.5
6.0
TIME (s)

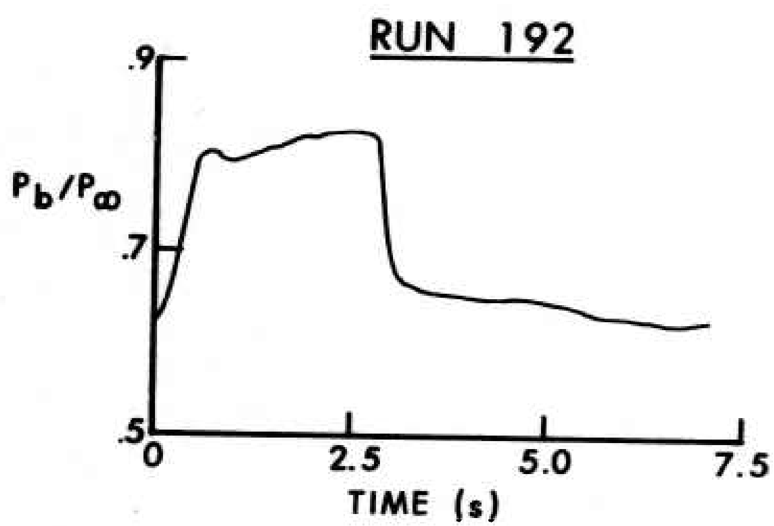
RUN 192
P_b/P_∞
.9
.7
.5
0
2.5
5.0
7.5
TIME (s)

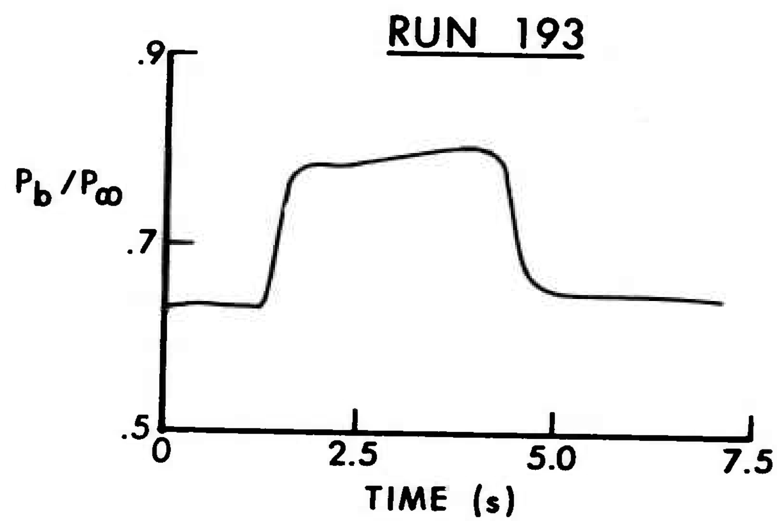
RUN 193
P_b/P_∞
.9
.7
.5
0
2.5
5.0
7.5
TIME (s)

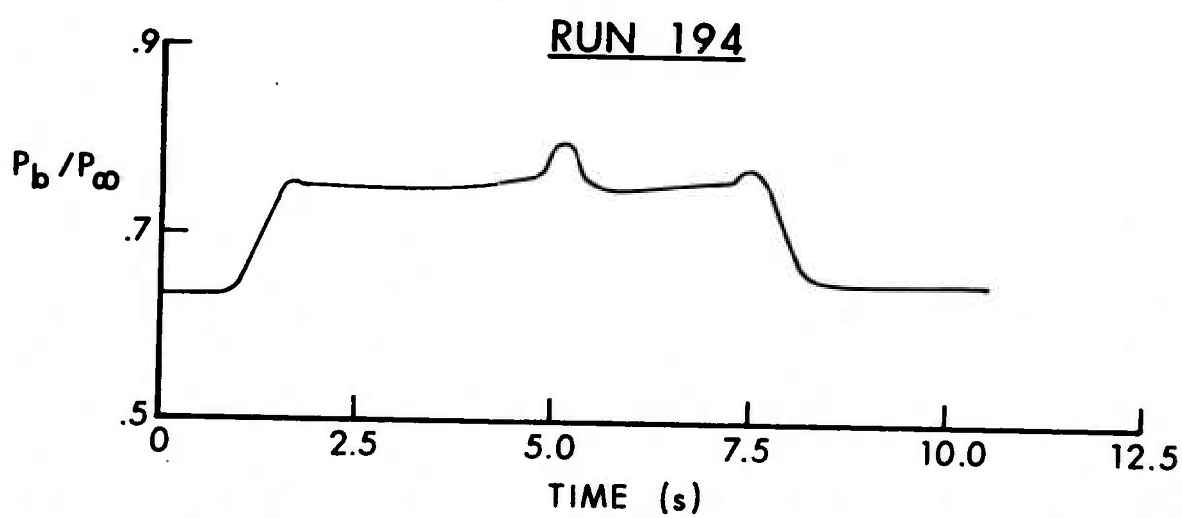
RUN 194
P_b/P_∞
.9
.7
.5
0
2.5
5.0
7.5
10.0
12.5
TIME (s)

DISTRIBUTION LIST

No. of Copies	Organization
2	Commander Defense Documentation Center ATTN: DDC-TCA Cameron Station Alexandria, VA 22314
1	Director Institute for Defense Analysis ATTN: Dr. H. Wolfhard 400 Army-Navy Drive Arlington, VA 22202
1	Commander US Army Materiel Development and Readiness Command ATTN: DRCDMA-ST 5001 Eisenhower Avenue Alexandria, VA 22333
1	Commander US Army Materiel Development and Readiness Command ATTN: DRCDE-A 5001 Eisenhower Avenue Alexandria, VA 22333
1	Commander US Army Materiel Development and Readiness Command ATTN: DRCDE-R 5001 Eisenhower Avenue Alexandria, VA 22333
1	Commander US Army Aviation Systems Command ATTN: DRSAV-E 12th and Spruce Streets St. Louis, MO 63166
1	Director US Army Air Mobility Research and Development Laboratory Ames Research Center Moffett Field, CA 94035
1	Commander US Army Electronics Command ATTN: DRSEL-RD Fort Monmouth, NJ 07703
4	Commander US Army Missile Command ATTN: DRSMI-R DRSMI-RK Dr. R. Rhoades Mr. N. White Redstone Arsenal, AL 35809
1	Commander US Army Tank Automotive Logistics Command ATTN: DRSTA-RHFL Warren, MI 48090
2	Commander US Army Mobility Equipment Research & Development Center ATTN: Tech Docu Cen, Bldg 315 DRSME-RZT Fort Belvoir, VA 22060
2	Commander US Army Armament Command ATTN: G. Fischer J. Turkeltaub/W. Romans Rock Island, IL 61202
7	Commander US Army Frankford Arsenal ATTN: SARFA-L1000 SARFA-J7200, C. Dickey R. Kwatnoski T. Elmendorf SARFA-J7100, G. Bornheim SARFA-J5300, W. Gadomski SARFA-8200, D. Mancinelli Philadelphia, PA 19137

DISTRIBUTION LIST

No. of Copies	Organization
7	Commander US Army Picatinny Arsenal ATTN: H. Hudgins D. Katz S. Kravitz J. Picard F. Taylor N. Weins D. Werbel Dover, NJ 07801
1	Commander US Army White Sands Missile Range ATTN: STEWS-VT White Sands, NM 88002
1	Commander US Army Harry Diamond Labs ATTN: DRXDO-TI 2800 Powder Mill Road Adelphi, MD 20783
1	Commander US Army Materials & Mechanics Research Center ATTN: DRXMR-ATL Watertown, MA 02172
1	Commander US Army Natick Laboratories ATTN: DRXRE, Dr. D. Sieling Natick, MA 01762
1	Director US Army TRADOC Systems Analysis Activity ATTN: ATAA-SA White Sands, NM 88002
2	Commander US Army Research Ofc (Durham) ATTN: Mr. R. Heaston Tech Lib P.O. Box 12211 Research Triangle Park NC 27709

No. of Copies	Organization
3	Commander US Naval Air Systems Command ATTN: AIR-604 Washington, DC 20360
3	Commander US Naval Ordnance Systems Command ATTN: ORD-0632 ORD-035 ORD-5524 Washington, DC 20360
1	Chief of Naval Research ATTN: ONR-429 Department of the Navy Washington, DC 20360
1	Commander US Naval Missile Center ATTN: Code 5632 Point Mugu, CA 93041
1	Commander US Naval Surface Weapons Center ATTN: Tech Lib Dahlgren, VA 22448
3	Commander US Naval Surface Weapons Center ATTN: Code 730 F. Baltakis S. Hastings Silver Spring, MD 20910
3	Commander US Naval Weapons Center ATTN: Code 608 Mr. J. Crump Code 753, Tech Lib Mr. J. Eisel China Lake, CA 93555
2	Commander US Naval Ammunition Depot ATTN: B. Douda J. Tanner Crane, IN 47522

DISTRIBUTION LIST

No. of Copies	Organization
1	Director US Naval Research Laboratory ATTN: Code 6180 Washington, DC 20390
2	Superintendent US Naval Postgraduate School ATTN: Tech Lib A. Fuhs Indian Head, MD 20640
1	AFSC (DOL) Andrews AFB Washington, DC 20331
1	AFOSR (SREP) 1400 Wilson Boulevard Arlington, VA 22209
2	AFRPL (RPMCP) ATTN: Dr. R. Weiss Dr. R. Schoner Edwards AFB, CA 93523
2	Headquarters, National Aeronautics and Space Administration ATTN: RPS; RP Washington, DC 20546
1	Director NASA Scientific & Technical Information Facility ATTN: CRT P.O. Box 8757 Baltimore/Washington International Airport, MD 21240
1	Director National Aeronautics and Space Administration George C. Marshall Space Flight Center ATTN: Tech Lib Huntsville, AL 35812
1	Director Jet Propulsion Laboratory ATTN: Tech Lib 4800 Oak Grove Drive Pasadena, CA 91103
1	Director National Aeronautics and Space Administration John F. Kennedy Space Center ATTN: Tech Lib Kennedy Space Center, FL 32899
1	Director National Aeronautics and Space Administration Langley Research Center ATTN: MS-185, Tech Lib Langley Station Hampton, VA 23365
2	Director National Aeronautics and Space Administration ATTN: MS-603, Tech Lib MS-86, Dr. Povinelli 21000 Brookpark Road Lewis Research Center Cleveland, OH 44135
1	Director National Aeronautics and Space Administration Manned Spacecraft Center ATTN: Tech Lib Houston, TX 77058
1	Aerojet Solid Propulsion Co. ATTN: Dr. P. Micheli Sacramento, CA 95813
1	ARO Incorporated ATTN: Mr. N. Dougherty Arnold AFS, TN 37389

DISTRIBUTION LIST

No. of Copies	Organization
1	Atlantic Research Corp. ATTN: Tech Lib Shirley Highway at Edsall Road Alexandria, VA 22314
1	Calspan Corporation P.O. Box 235 Buffalo, NY 14221
1	Dow Chemical Company ATTN: George Lane Midland, MI 48640
1	Explosives Corp. of America ATTN: Patrick A. Yates P.O. Box 906 Redmond, WA 98052
1	General Electric Company Flight Propulsion Division ATTN: Tech Lib Cincinnati, OH 45215
2	Hercules Incorporated Alleghany Ballistic Labs ATTN: Dr. R. Yount Tech Lib Cumberland, MD 21501
1	Hercules Incorporated Bacchus Division ATTN: Dr. M. Beckstead Magna, UT 84044
1	Lockheed Palo Alto Rsch Labs ATTN: Tech Info Ctr 3251 Hanover Street Palo Alto, CA 94304
1	Lockheed Propulsion Company ATTN: Dr. N. Cohen P.O. Box 111 Redlands, CA 92373

No. of Copies	Organization
1	McDonnell Douglas Corp Missile & Space Sys Div ATTN: Tech Lib Santa Monica, CA 90406
1	The Marquardt Corporation ATTN: Tech Lib P.O. Box 2013 Van Nuys, CA 91404
1	The Martin-Marietta Corporation Denver Division ATTN: Res Lib P.O. Box 179 Devner, CO 80201
1	MB Associates ATTN: Dr. A. McCone San Ramone, CA 94583
2	North American Rockwell Corp. Rocketdyne Division ATTN: Dr. C. Oberg Tech Lib 6633 Canoga Avenue Canoga Park, CA 91304
2	North American Rockwell Corp. Rocketdyne Division ATTN: Mr. W. Haymes Tech Lib McGregor, TX 76657
3	Thiokol Chemical Corporation Huntsville Division ATTN: Dr. D. Flanigan Tech Lib E. Barnes Huntsville, AL 35807
1	Thiokol Chemical Corporation Longhorn Division ATTN: Dave Dillehay Marshall, TX 79843

DISTRIBUTION LIST

No. of Copies	Organization
3	Thiokol Chemical Corporation Wasatch Division ATTN: Dr. M. Mihlfeith Graham Shaw Tech Lib P.O. Box 524 Brigham City, UT 84302
1	TRW Systems Group ATTN: Mr. H. Korman One Space Park Redondo Beach, CA 90278
1	United Aircraft Corporation Pratt and Whitney Division ATTN: Tech Lib P.O. Box 2691 West Palm Beach, FL 33402
1	United Aircraft Corporation Research Laboratories ATTN: Dr. R. Waesche East Hartford, CT 06108
2	United Technology Center ATTN: Dr. R. Brown Tech Lib P.O. Box 358 Sunnyvale, CA 94088
1	Battelle Memorial Institute ATTN: Tech Lib 505 King Avenue Columbus, OH 43201
2	Brigham Young University Dept of Chemical Engineering ATTN: Prof R. Coates Prof M. Horton Provo, UT 84601
2	California Institute of Tech ATTN: Prof F. Culick Tech Lib 1201 East California Boulevard Pasadena, CA 91102

No. of Copies	Organization
1	Case Western Reserve University Division of Aerospace Sciences ATTN: Prof J. Tien Cleveland, OH 44135
4	Georgia Institute of Technology School of Aerospace Engineering ATTN: Prof B. Zinn Prof W. Strahle S. Pronchick Prof E. Price Atlanta, GA 30333
1	IIT Research Institute ATTN: Prof T. Torda 10 West 35th Street Chicago, IL 60616
1	Director Applied Physics Laboratory The Johns Hopkins University ATTN: Dr. R. Centrell Johns Hopkins Road Laurel, MD 20810
2	Director Chemical Propulsion Information Agency The Johns Hopkins University ATTN: Mr. T. Christian Tech Lib Johns Hopkins Road Laurel, MD 20810
1	Massachusetts Institute of Technology Dept of Mechanical Engineering ATTN: Prof G. Faeth University Park, PA 16802
3	Princeton University Dept of Aerospace and Mechanical Sciences ATTN: Prof M. Summerfield Prof I. Glassman Tech Lib James Forrestal Campus Princeton, NJ 08540

DISTRIBUTION LIST

No. of Copies	Organization
7	Purdue University School of Mechanical Engineering ATTN: Prof J. Osborn Prof S. N. B. Murthy John Andrews Duane Baker Prof B. A. Reese Harry Bruestle Prof D. E. Abbott Lafayette, IN 47907
1	Rutgers-State University Dept of Mechanical and Aerospace Engineering ATTN: Prof S. Temkin University Heights Campus New Brunswick, NJ 08903
1	Stanford Research Institute Propulsion Sciences Division ATTN: Tech Lib 333 Ravenswood Avenue Menlo Park, CA 94204
1	Stevens Institute of Technology Davidson Laboratory ATTN: Prof R. McAlevy III Hoboken, NJ 07030
2	University of California Dept of Aerospace Engineering ATTN: Prof S. Penner Prof F. Williams La Jolla, CA 92037

No. of Copies	Organization
2	University of Denver Denver Research Institute ATTN: R. M. Blunt Tech Lib P.O. Box 10127 Denver, CO 80210
2	University of Illinois Dept of Aeronautical Engineering ATTN: Prof H. Krier Prof R. Strehlow Urbana, IL 61803
1	University of Minnesota Dept of Mechanical Engineering ATTN: Prof E. Fletcher Minneapolis, NM 55455
2	University of Utah Dept of Chemical Engineering ATTN: Prof A. Baer Prof G. Flandro Salt Lake City, UT 84112

Aberdeen Proving Ground

Marine Corps Ln Ofc
Dir, USAMSAA